Revisiting *peri*-aryloxyquinones: From a forgotten photochromic system to a promising tool for emerging applications

Andrey G. Lvov[a,b,]*, Lyubov S. Klimenko[c], Vasily N. Bykov[a,b], Stefan Hecht[d,e,]*

[a] *A. E. Favorsky Irkutsk Institute of Chemistry, Siberian Branch of the Russian Academy of Sciences 1 Favorsky St., Irkutsk, 664033, Russia. E-mail:* *lvov-andre@yandex.ru*

[b] *Irkutsk National Research Technical University 83, Lermontov St., Irkutsk, 664074, Russia*

[c] *Yugra State University, 16 Chekhov St., Khanty-Mansiysk, 628012, Russia*

[d] *Department of Chemistry & Center for the Science of Materials Berlin, Humboldt-Universität zu Berlin, Brook-Taylor-Str. 2, 12489 Berlin, Germany. E-mail:* *sh@chemie.hu-berlin.de*

[e] *DWI – Leibniz Institute for Interactive Materials, Forckenbeckstr. 50, 52074 Aachen, Germany*

in memory of Professor Valery Barachevsky
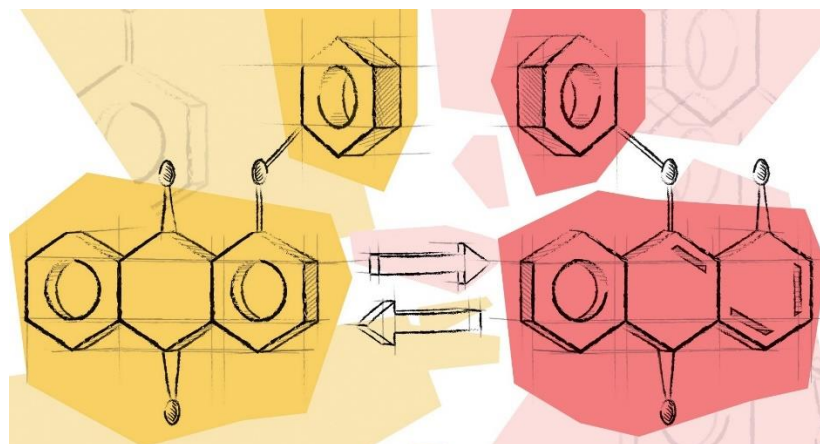
Abstract

Emerging applications of photochromic compounds demand new molecular designs that can be inspired by some long-known yet currently forgotten classes of photoswitches. In the present review, we would like to remind the community about *Peri*-AryloxyQuinones (PAQs) and their unique photoswitching behavior originally discovered by Gerasimenko more than 50 years ago. At the heart of this phenomenon is the light-induced migration of an aromatic moiety (arylotropy) in *peri*-aryloxy-substituted quinones resulting in *ana*-quinones. PAQs feature absorbance of both

1

isomers in the visible spectral region, photochromism in the amorphous and crystalline state, and thermal stability of the photogenerated *ana*-isomer. Particularly noticeable is the high sensitivity of the *ana*-isomer towards nucleophiles in solution. In addition to the mechanism of molecular photochromism and the underlaying structure-switch relationships, we analyze potential applications and prospects of aryloxyquinones in optically switchable materials and devices. Due to their ability to efficiently photoswitch in the solid state, PAQs are indeed attractive candidates for such materials and devices, including electronics (optically controllable circuits, switches, transistors, memories, and displays), porous crystalline materials, crystalline actuators, photoactivated sensors, and many more. This review is intended to serve as a guide for researchers who wish to use photoswitchable PAQs in the development of new photocontrollable materials, devices, and processes.

Table of Contents

I. Introduction

Photochromism is a reversible isomerization of a chemical species under the action of light to produce a metastable photoinduced state (Figure 1).[1] The distinction between the structures of the initial compound and its photoisomer determine their different physical and chemical properties (color, conductance, acidity/basicity, redox potentials, chemical and biological activity, etc). The peculiarities of light (high spatio-temporal resolution, tenability of energy and intensity) make photoswitches attractive components for new materials and technologies.[2] Traditionally, photochromic compounds were considered as a basis for memory devices.[3] During the past decade, a vast number of new applications of photoswitches in photopharmacology and biomedicine,[4,5] catalysis,[6] additive manufacturing,[7] renewable energetics,[8] and molecular electronics,[9] porous crystalline materials,[10] crystal actuators,[11] liquid crystal polymer networks,[12] and supramolecular chemistry[13] emerged. A variety of applications require a wide range of molecular instruments, the most popular of which include diarylethenes,[14] fulgides,[15] azobenzenes,[16] and spiropyranes/spiroxazines (Figure 1).[17] In addition to these classes, in the past decades a number of new classes[18] were elaborated, such as donor-acceptor Stenhouse adducts (DASAs),[19] diazocines,[20] hydrazones,[21] iminothioindoxyls,[22] hemipiperazines,[23] and homoaromatic hydrocarbons.[24] At the same time, revision of some classes of photoswitches was carried out, for example, indigo and their analogs,[25] hemiindigo,[26] and dihydropyrene[27] derivatives, acenes,[28] stilbenes,[29,30] and bisimidazole derivatives.[31]

The photogenerated, metastable isomers revert back under irradiation or thermally. The latter is governed by the thermal stability of the photogenerated isomer that historically has been used to divide photochromic molecules into two groups. Compounds that form thermally unstable photoisomers (with thermal half-lives, $t_{1/2}$, ranging from milliseconds or seconds to days) display so called T-type photochromism, whereas photoswitches with thermally stable photoisomers (with $t_{1/2}$ of months or years) exhibit P-type photochromism. Thermal stability is a key property and largely defines specific applications of photochromic compounds. Despite the great variety of photoswitchable molecules (Figure 1, left), thermally irreversible photoswitches are still mainly limited to diarylethenes and fulgides.

Another crucial requirement for many applications is related to effective and efficient photoswitchability in the solid state. The geometry changes imposed upon light-induced isomerization often limit the photoreactivity of a molecule, in particular in highly ordered liquid crystalline and crystalline solids.[32,33] Overall, a transition from solutions and polymeric films as media for photoswitching performance towards highly ordered and crystalline states has been realized in recent years[2a] and photoswitches have successfully been used in a variety of solid-state

3

applications, including electronic devices (transistors, memories, displays), photoswitchable metal−organic frameworks, and crystalline actuators (Figure 1, right).
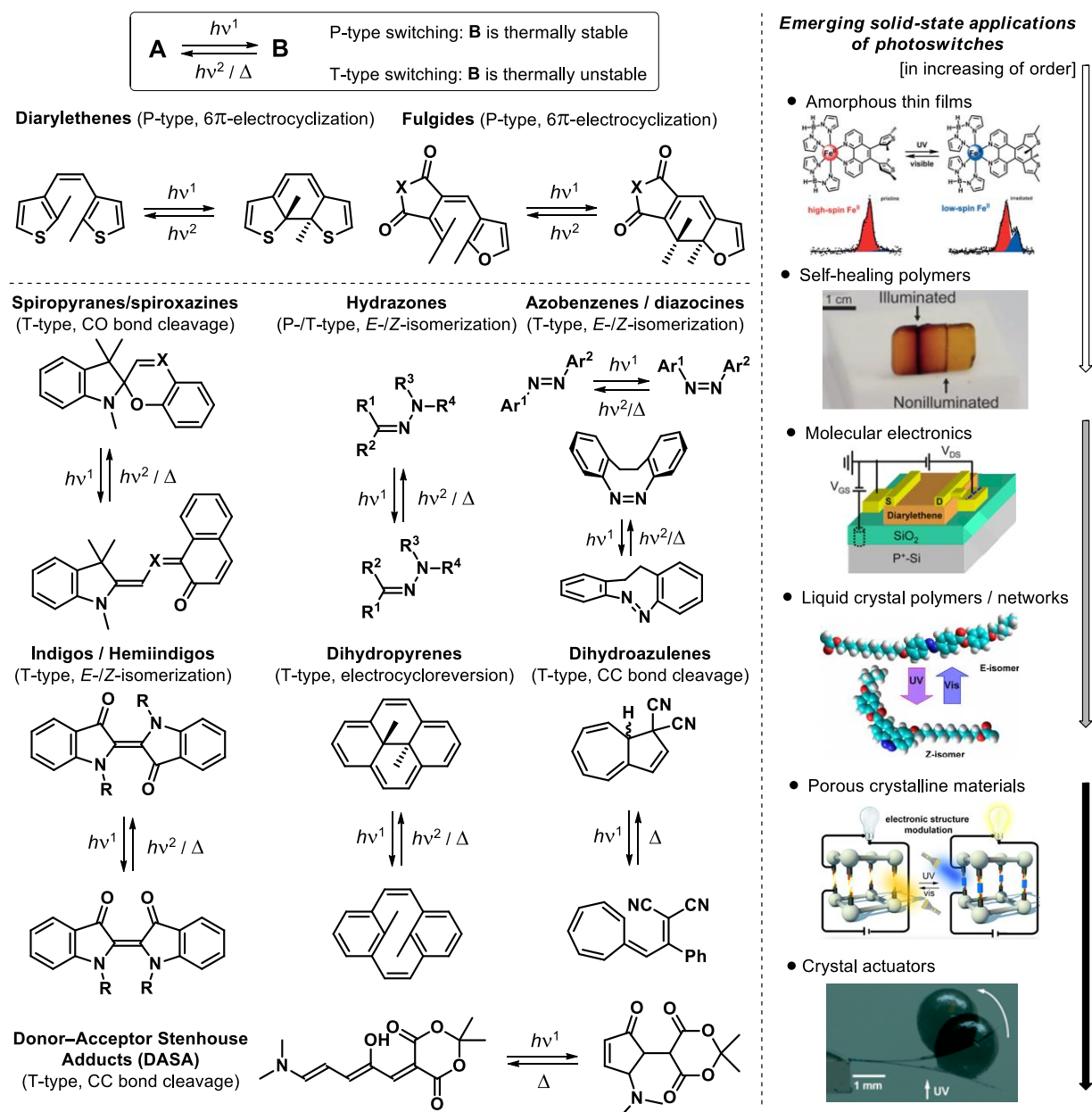

Figure 1. Various classes of photoswitchable compounds and some emerging applications. Adapted from refs. [34], [35], [36], [37], [38], [39] with permission of the American Chemical Society and Wiley.

The overwhelming majority of the known classes of photoswitches employs cyclization/cycloreversion or *E*/*Z* isomerization processes (Figure 1). One exception based on another switching mechanism, namely, photoinduced arylotropy, was reported for *peri*-aryloxyquinones (PAQs). The light-induced phenomenon was discovered by Gerasimenko *et al.* in 1971 for the simplest 1-phenoxyanthraquinone, *para*-**1** (Figure 2).[40] Irradiation of *para*-**1** with

4

UV or violet light resulted in migration of the phenyl group from the oxygen atom in position 1 (α) to the adjacent carbonyl group in position 9 (*meso*) to give *ana*-substituted 9-phenoxy-1,10-anthraquinone.[41] *Para*-**1** and its derivatives display a positive photochromic behavior with absorbance of both isomers in the visible region (Figure 2A) and photochromism occurring in the solid state (yellow crystalline *para*-**1** changes its color to orange under UV light[40]). From the available data *para*-**1** can be considered as a P-type photoswitch. Thus, PAQs represent a rare class of visible light-driven, thermally stable photoswitches operating in the solid state.
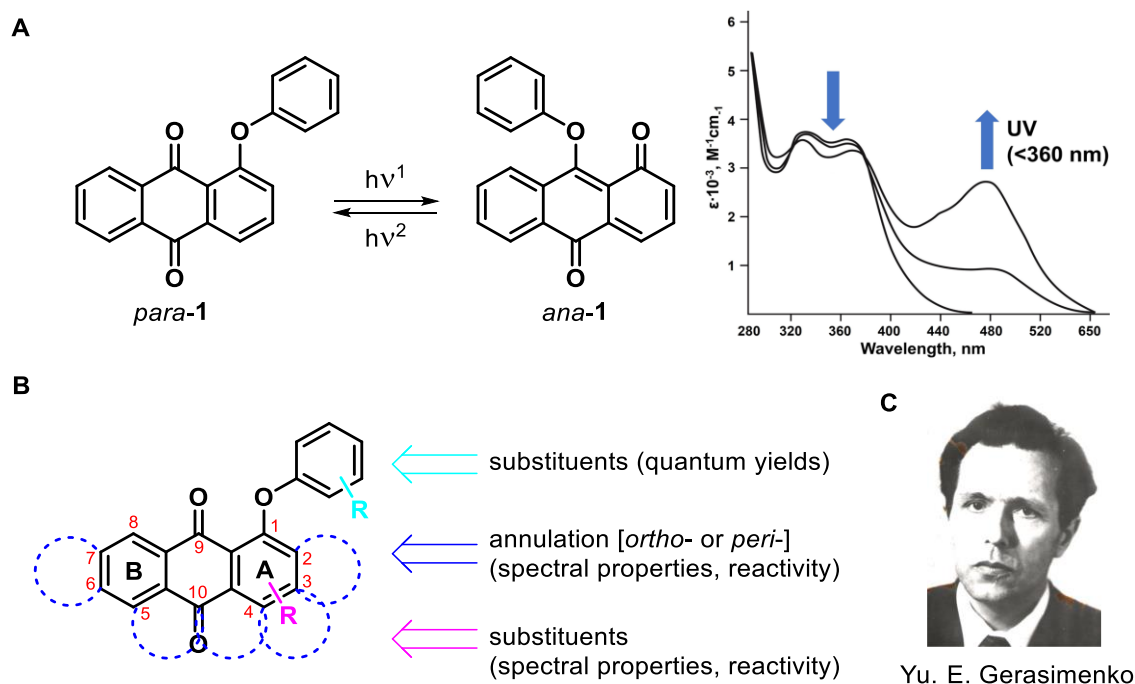

Figure 2. Photochromic behavior of the simplest PAQ, *para*-**1** (A, left) and spectral changes of *para*-**1** in benzene upon UV irradiation (A, right). Chemical approaches to modify the structure of *para*-**1** (B). Yu. E. Gerasimenko (1931-1986) – a pioneer of photoswitchable PAQs (C).

In 1970s and 1980s the effect of the PAQ structure on the spectral properties and some switching characteristics were investigated. These results were summarized by Gerasimenko,[42] Sokolyuk et al.,[43] Gritsan,[44] as well as Barachevsky[45,46] during the 1990s. The emergence of new applications for photochromic molecules over the past two decades and the associated challenges suggests to revisit *peri*-aryloxyquinones and take a fresh look at the capabilities and limitations of this class of photoswitches. Our present review should become a guide for researchers who intend to explore and utilize PAQ molecules for the development of photoswitchable molecules, materials, and devices.

5

II. Photochromic Performance

In this section, we describe how the molecular structure of *peri*-aryloxyquinones affects the most important photoswitching parameters, including absorption spectra, quantum yields, photoconversion and photoactivity as well as fatigue resistance. Spectral properties (absorption maxima and extinction coefficients) of the initial and photogenerated isomers of any class of photochromic compounds define the addressability of the molecules by light of a certain wavelength, from the high-energy UV to the low energy red and NIR region.[47] Quantum yields provide a measure for the efficiency of photoinduced processes. Photoconversion depends on both the selective excitation and the associated quantum yield. In the photostationary state (PSS), the ratio of both isomers depends on the ratio of their extinction coefficients and the ratio of the quantum yields for forward and backward reaction at the given wavelength.[48] As photochromic activity, we consider the presence or absence of a photochromic reaction under the given conditions. Last but not least, fatigue resistance refers to the ability of the photochromic system to be operated many times without photodegradation.

Three possible approaches to modulate the PAQ's properties are discussed (Figure 2B): Annulation (*ortho*-annulation is the installment of a new ring at the 2,3- or 3,4-positions; *peri*-approach[49] adds a new ring at the 4,10- or 5,10-positions) and introduction of functional groups in the benzene rings A and B as well as the migrating aryl group.

II.1. Spectral properties

PAQ photoswitches display positive photochromism. Their thermodynamically more stable *para*-isomers usually exhibit absorption maxima in the UV or visible region (Figure 3). The parent photoswitchable aryloxyquinone **1** displays an already relatively long wavelength absorbance of its *para*-isomer with a maximum at 364 nm and maximum of its *ana*-isomer at 480 nm. Further tuning of spectral properties is possible by means of substitution or annulation of ring A (see Figure 2B). At the same time, substituents on the migrating aryl group only weakly affect the maxima of absorption bands of both *para*- as well as *ana*-isomers.[50,51,52] In general, PAQ photoswitches exhibit a significant band separation of their *para*- and *ana*-isomers as a result of the fully aromatic π-system in the *para*-isomers formally consisting of two benzene rings while the *ana*-isomers consists of only one benzene ring and a system of conjugated double bonds.
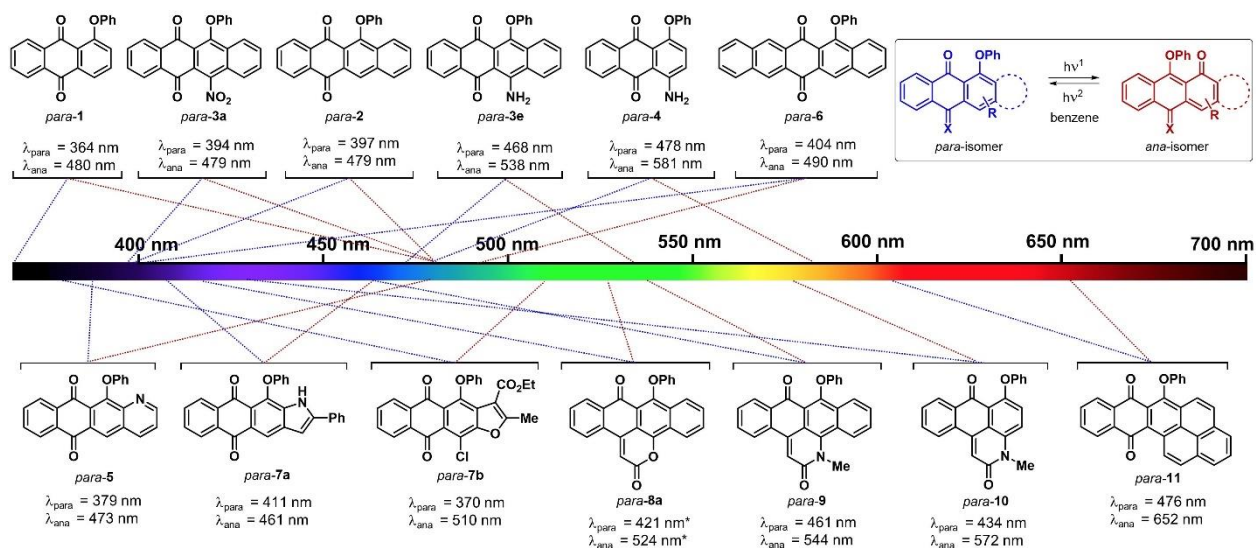
6

Figure 3. Spectral properties of selected PAQ photoswitches: Absorption maxima of *para*- and *ana*-isomers in toluene/benzene (* in DMSO).

Effect of ring A *ortho*-annulation. The photochromic transformations and spectral changes of *para*-**12a** until reaching the PSS upon UV irradiation as well as its reverse isomerization upon visible light irradiation are shown in Figure 4A. Both processes feature clean isosbestic points as the result of bimolecular reactions without significant byproduct formation (photodegradation). Comparison of spectral properties of PAQs **1** and **2**[53] shows, that the benzannulation of ring A led to a bathochromic shift of the *para*-isomer absorption (from 364 nm to 397 nm), while the λ_{max} of the *ana*-isomers remains unchanged. At the same time, the shape of the low energy band changes significantly. Unlike the parent aryloxyanthraquinone *para*-**1**, its annulated derivatives form *ana*-isomers possessing maxima with a distinct vibrational fine structure. Thus, *ana*-**12a** features a prominent band in the visible region with maxima at 450 nm and 478 nm.[52]

Ring A *ortho*-annulation of *para*-**1** by *N*-containing heterocycles (pyridine for *para*-**5**[54] and pyrrole for *para*-**7a**[55]) results in a bathochromic shift of the *para*-isomer as well as a hypsochromic shift of the photogenerated isomer. For *para*-**7a**, the absorption maximum reaches the visible region ($\lambda_{max} = 411$ nm in benzene). Annulation by furan has the opposite effect and the corresponding *para*-**7b** has a red-shifted maximum of the *ana*-form at 510 nm.[56]
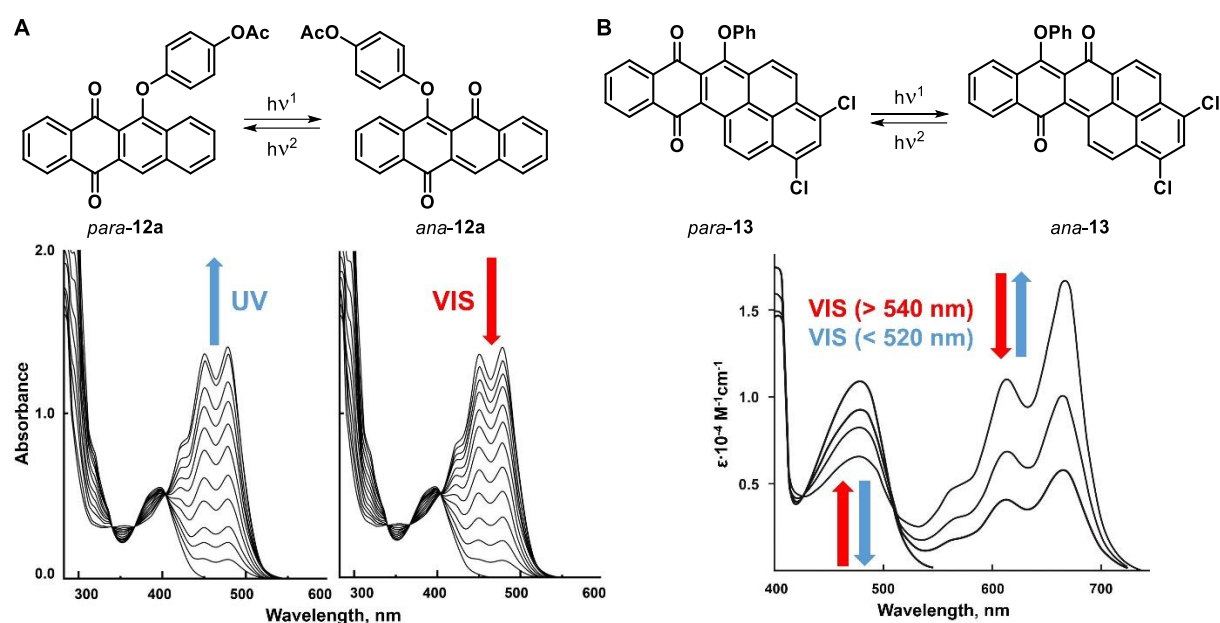
7

Figure 4. Photochromic reaction and spectral changes of *para*-**12a** in toluene upon UV irradiation (λ^{irr} = 365 nm, left) and subsequent visible light irradiation (λ^{irr} = 505 nm, right) (B). Photochromic reaction and spectral changes of *para*-**13** under visible light irradiation in chlorobenzene (B). Adapted with permission from ref. [52]. Copyright 1996 Chemical Society of Japan.

Effect of ring B *ortho*-annulation. Addition of a benzene to ring B of **2** gave 5-phenoxy-6,13-pentacenequinone *para*-**6** with slightly bathochromically shifted (7-11 nm) maxima of both photoisomers.[57]
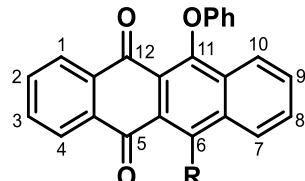
Effect of double ring A *ortho*-annulation. The π-extension of ring A by three additional benzene rings[50] greatly shifts the maxima of both photoisomers to the red spectral region for 2,3-phthaloylpyrene derivative *para*-**11**. The orange *para*-isomer has a maximum at 476 nm and the corresponding *ana*-isomer at 652 nm. Spectral changes for analogue *para*-**13** are presented in Figure 4B. It should be noted, that multiple annulations by benzene rings are a reliable approach for red-shifted photoswitches, as was demonstrated recently by Dube and coworkers for *peri*-anthracenethioindigo derivatives.[58]

Effect of *peri*-annulation. Addition of heterocyclic rings (pyranone, 2-pyridone or pyridine) at the 4,10- or 5,10-positions of *para*-**1** and *para*-**2** also leads to a remarkable red-shift of the absorption of both isomers. For example, *para*-**9** and *ana*-**9** absorb at 461 nm and 544 nm, respectively.[59]

Effect of ring A substitution. Introduction of various substituents at the ring A of *para*-**2** provides an opportunity to change the absorption properties (Chart 1).[60] The most pronounced effect was reported when amino and acylamino groups were introduced. In these cases, the maxima of the
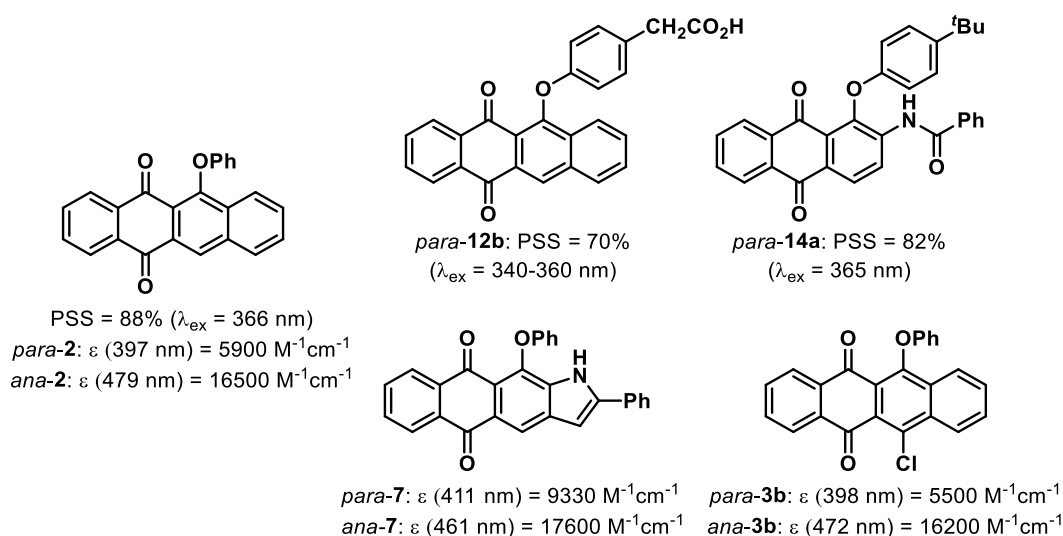
8

para-isomers were shifted bathochromically from 400 nm to 429 nm and 468 nm, respectively, with similar red-shifts of the *ana*-isomers.

Chart 1. Spectral properties of 6-substituted naphthacenequinone PAQs.

		λ (*para-*)	λ (*ana-*)
3a (R = NO$_2$):		394 nm	479 nm
3b (R = Cl):		398 nm	472 nm
2 (R = H):		397 nm	479 nm
3c (R = OMe):		400 nm	469 nm
3d (R = NHAc):		429 nm	504 nm
3e (R = NH$_2$):		468 nm	538 nm

Quantifying spectral properties and PSS composition of *ana*-isomers. During light exposure, common photoswitches rarely achieve a quantitative conversion (100%) to the light-generated state due to reaching the PSS, in which the rates of forward and back photoreactions are equal. The conversion of the *para*-isomer to the *ana*-isomer in the PSS was reported for a number of PAQs (Chart 2). For *para*-**2** this value was as high as 88% in toluene upon 366 nm irradiation.[52] Comparable conversions were reported for *para*-**12b**[61] and *para*-**14a**.[62] Thus, PAQs feature quite high photoconversions between their isomers. Due to its elongated π-system, the *ana*-isomers exhibit higher extinction coefficients than their *para*-counterparts. For example, *para*-**2** exhibits ε = 5900 M^{-1}cm^{-1} whereas *ana*-**2** has ε = 16500 M^{-1}cm^{-1}.[63] Comparable values were obtained for PAQ **3b**, while for *ana*-**7** the extinction coefficient was as high as 17600 M^{-1}cm^{-1}.

Chart 2. PSS conversions and extinction coefficients for some PAQs in toluene (*para*-**12b** in DMSO).

PSS = 88% (λ$_{ex}$ = 366 nm)
para-**2**: ε (397 nm) = 5900 M^{-1}cm^{-1}
ana-**2**: ε (479 nm) = 16500 M^{-1}cm^{-1}

para-**12b**: PSS = 70%
(λ$_{ex}$ = 340-360 nm)

para-**14a**: PSS = 82%
(λ$_{ex}$ = 365 nm)

para-**7**: ε (411 nm) = 9330 M^{-1}cm^{-1}
ana-**7**: ε (461 nm) = 17600 M^{-1}cm^{-1}

para-**3b**: ε (398 nm) = 5500 M^{-1}cm^{-1}
ana-**3b**: ε (472 nm) = 16200 M^{-1}cm^{-1}

9

The evaluation of photoconversion at PSS and, hence, extinction coefficients of photogenerated isomers, requires an additional analytical method such as ^{1}H NMR or HPLC along with UV-Vis spectroscopy. Krongauz and coworkers suggested an ingenious method to determine this value by trapping the *ana*-isomer in an irreversible reaction with amines (see Section II.6 for details).[64] Addition of excess of decylamine[64] or ammonia[65] to the PSS solution of PAQs resulted in instant formation of a colored product with an absorption maximum, different from the *ana*-isomer (Figure 5). Further irradiation converted the remaining *para*-isomer via the corresponding *ana*-isomer to the amine adduct. For *para*-**18** conversion as high as 83% was determined both in toluene and DMSO.
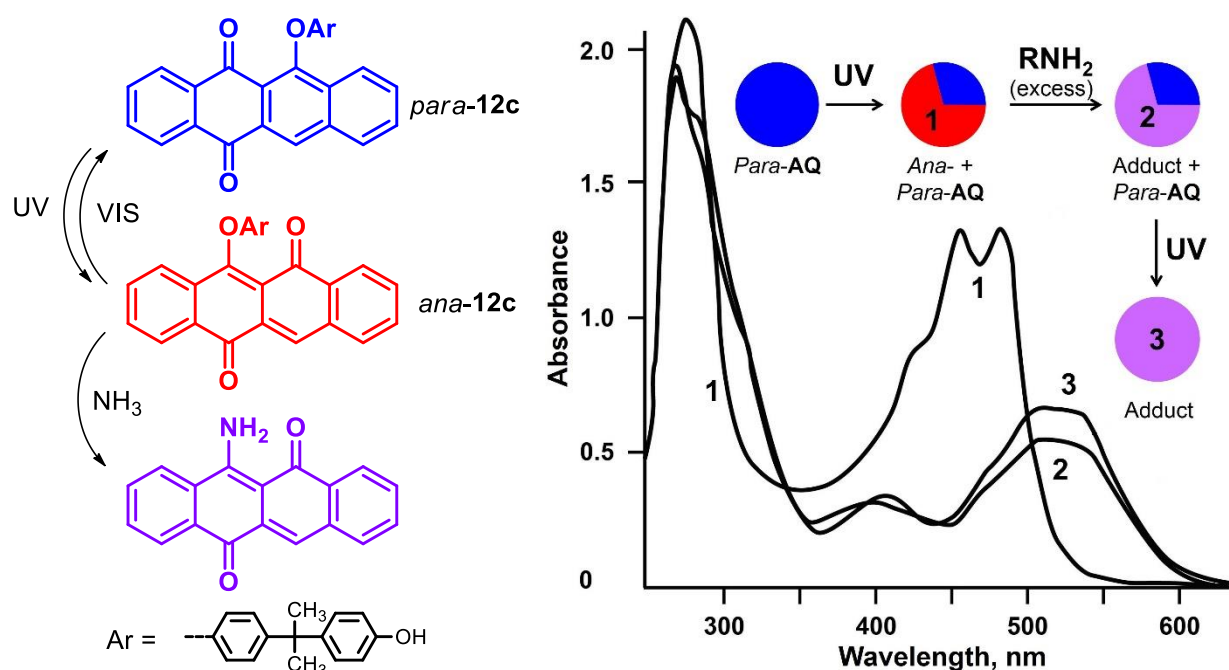

Figure 5. Evaluation of PSS conversion of PAQ *para*-**12c** using irreversible reaction with amines. Absorbance of PAQ at PSS after UV irradiation (spectrum 1); after addition of excess of ammonia (spectrum 2) and after subsequent UV irradiation (spectrum 3). Adapted from ref. [65] with permission of Elsevier.

II.2. Effect of annulation and substitution on switchability

Annulation. In the original work, the photoswitching of 1,4-benzoquinone derivatives (anthraquinone, naphthacenequinone, etc) was successfully demonstrated. Afterwards, related compounds comprised of only one carbonyl in the switching chromophore were investigated (Chart 3). *Peri*-annulation of rings A or B and 1,4-benzoquinone with pyridone and pyridine

10

resulted in photoactive compounds: 6-phenoxyanthrapyridones *para*-**15**, 8-phenoxyanthrapyridone *para*-**16**, 9-phenoxynaphthacenepyridone *para*-**9**, as well as 6-phenoxy- and 8-phenoxyanthrapyridines *para*-**17** and *para*-**18**, respectively.[59,66] Heterocyclic derivatives were also found to be photoactive: 9-phenoxynaphthaceno[5,6-*bc*]pyran-2,8-dione *para*-**8a**[67] and 9-phenoxy-10*H*-benzo[*c*]naphtho[1,2,3-*mn*]acridin-10-one **20**.[68] Among pyrazoloanthrones[69] and pyrazolonaphtacenones,[70] *N*-acetylated derivatives **21** and **22** displayed the most pronounced photoswitching.

Chart 3. Photoactivity of *peri*-annulated PAQ derivatives. Absorption maxima are given in the toluene.
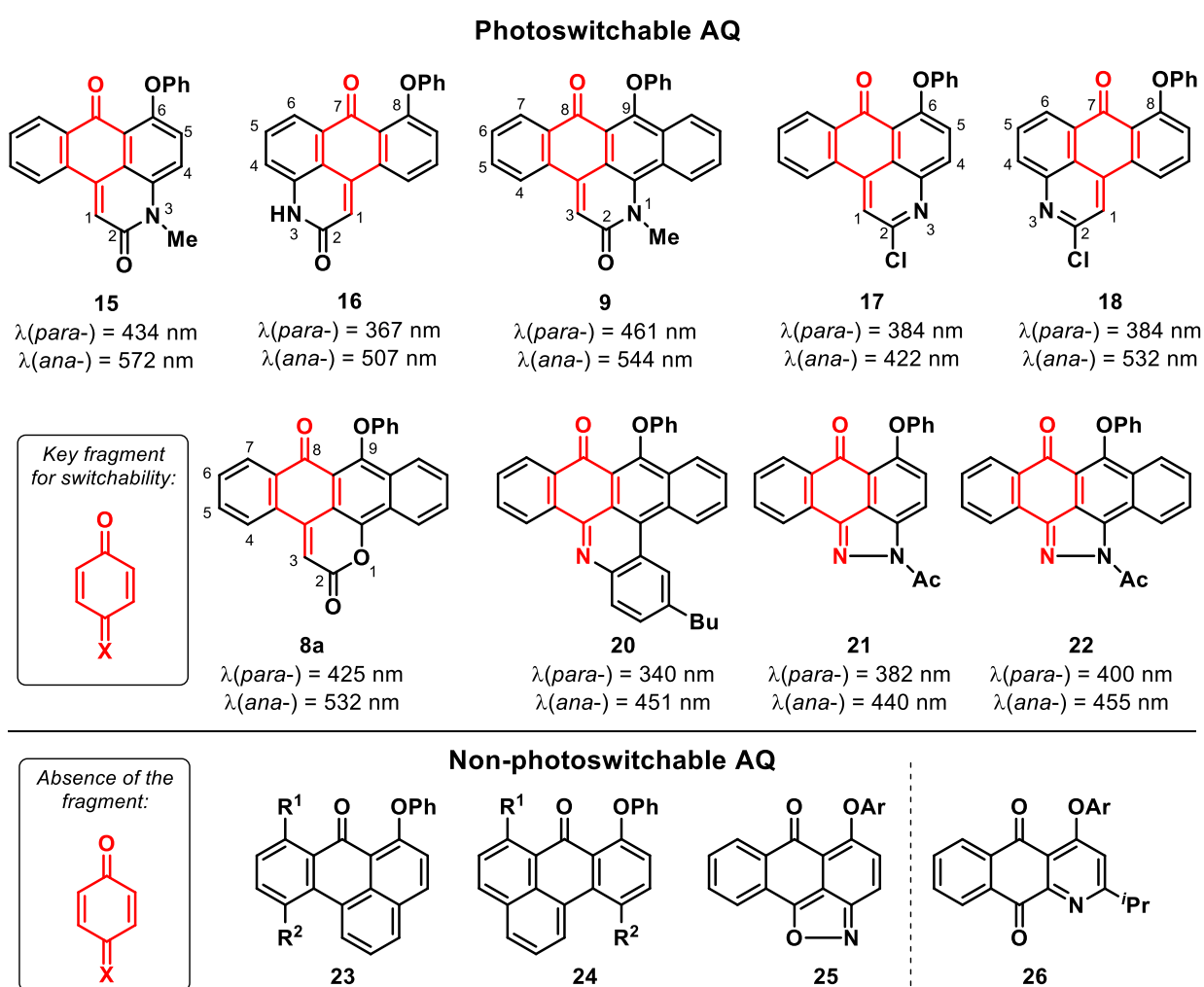
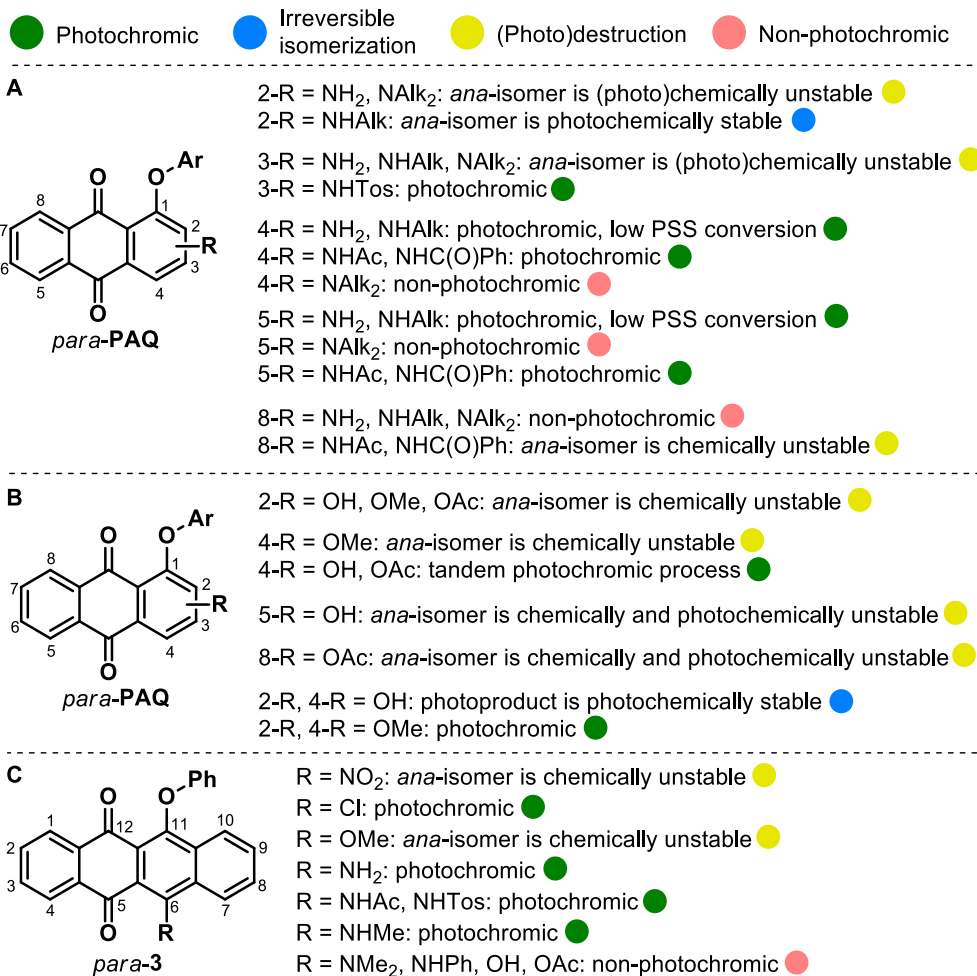Importantly, annulation that does not contribute to the central 1,4-quinone motif in PAQs prevents their switchability. Thus, the presence of aromatic benzene ring with high delocalization ability as *peri*-annulating motif results in photoinactive compounds **23** and **24**.[71] The same result was reported for isoxazole-based derivative **25**.[72] The benzo[*g*]quinoline-5,10-dione derivative **26**

11

was highly unstable under UV light in comparison with its analogue *para*-**5** (Figure 3), where an additional benzene ring divides the quinone and pyridine parts.[73]

Substitution. The effect of various substituents in the rings A and B on the photoactivity and photostability was studied in numerous papers for: 2,4,5-amino-substituted anthraquinone PAQs,[74] 2-amino-substituted anthraquinone PAQs,[75,76] 3,4,5,8-amino-substituted anthraquinone PAQs,[77] 2,4,5,8-oxy-substituted anthraquinone PAQs,[78] and 6-substituted naphthacenequinone PAQs.[60] The obtained substitution-switching relationships were not quantitative; however, they could be useful for choosing the appropriate switches for various applications. Depending on the nature and position of the substituents, the derived PAQs could be photochromic or non-photochromic, and show irreversible isomerization and/or (photo)degradation and/or pronounced chemical instability due to hydrolysis (Chart 4). In the series of anthraquinone PAQs, introduction of non-substituted amino groups in positions 2, 3 or 8 results in non-photochromic compounds or photoswitches with poor reversibility. An exception were 4- and 5-substituted derivatives. In this case, the primary photoproduct of 4-amino(hydroxy, acyloxy)-substituted PAQs undergoes additional thermal migration of either a hydrogen or acyl-group with formation of thermally and chemically stable 1,4-benzoquione derivatives (for details, see Section II.6.1).

Alkylation of the corresponding PAQs usually deteriorates the switching performance. On the contrary, acylation or tosylation of amino groups reduces the photoactivity and the corresponding PAQs are mostly photoswitchable. Installation of hydroxy groups usually led to compounds with poor switchability. Note, however, that 4-OH and 4-OAc derivatives show tandem photoisomerization process (see also section II.6.1).

Chart 4. Modes of substituted PAQ's photoactivity.

🟢 Photochromic 🔵 Irreversible isomerization 🟡 (Photo)destruction 🔴 Non-photochromic

- -

A

para-**PAQ**

2-R = NH_2, $NAlk_2$: *ana*-isomer is (photo)chemically unstable 🟡
2-R = NHAlk: *ana*-isomer is photochemically stable 🔵

3-R = NH_2, NHAlk, $NAlk_2$: *ana*-isomer is (photo)chemically unstable 🟡
3-R = NHTos: photochromic 🟢

4-R = NH_2, NHAlk: photochromic, low PSS conversion 🟢
4-R = NHAc, NHC(O)Ph: photochromic 🟢
4-R = $NAlk_2$: non-photochromic 🔴

5-R = NH_2, NHAlk: photochromic, low PSS conversion 🟢
5-R = $NAlk_2$: non-photochromic 🔴
5-R = NHAc, NHC(O)Ph: photochromic 🟢

8-R = NH_2, NHAlk, $NAlk_2$: non-photochromic 🔴
8-R = NHAc, NHC(O)Ph: *ana*-isomer is chemically unstable 🟡

- -

B

para-**PAQ**

2-R = OH, OMe, OAc: *ana*-isomer is chemically unstable 🟡

4-R = OMe: *ana*-isomer is chemically unstable 🟡
4-R = OH, OAc: tandem photochromic process 🟢

5-R = OH: *ana*-isomer is chemically and photochemically unstable 🟡

8-R = OAc: *ana*-isomer is chemically and photochemically unstable 🟡

2-R, 4-R = OH: photoproduct is photochemically stable 🔵
2-R, 4-R = OMe: photochromic 🟢

- -

C

para-**3**

R = NO_2: *ana*-isomer is chemically unstable 🟡
R = Cl: photochromic 🟢
R = OMe: *ana*-isomer is chemically unstable 🟡
R = NH_2: photochromic 🟢
R = NHAc, NHTos: photochromic 🟢
R = NHMe: photochromic 🟢
R = NMe_2, NHPh, OH, OAc: non-photochromic 🔴

An interesting phenomenon was reported for 2-monoalkylamino- and 2,4-dihydroxy substituted PAQs, consisting in irreversible photoswitching, e.g. formation of a photostable colored *ana*-isomer (Scheme 6).[75,76] Yellow solutions of these compounds turned blue upon light irradiation with formation of the corresponding *ana*-isomers. These products could be isolated from irradiated solutions in high yields.[76]
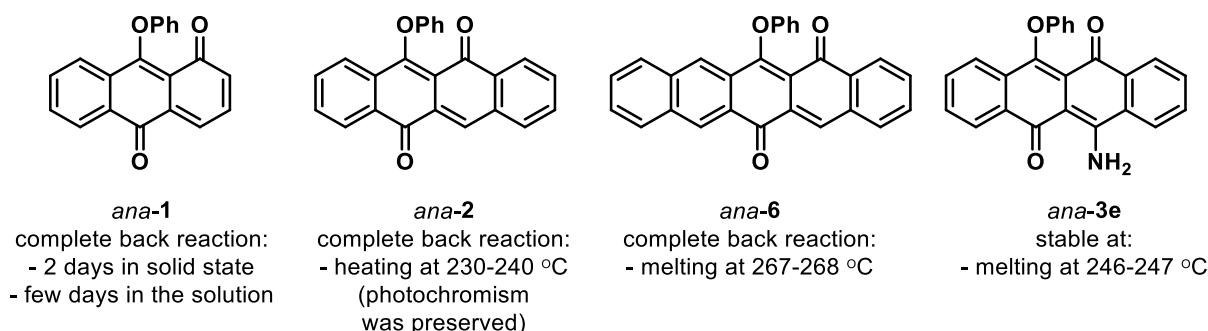
Scheme 6. Irreversible photoisomerization of 2-monoalkyl-substituted PAQ.

para-**27**
(yellow)

ana-**27**
(blue)

13
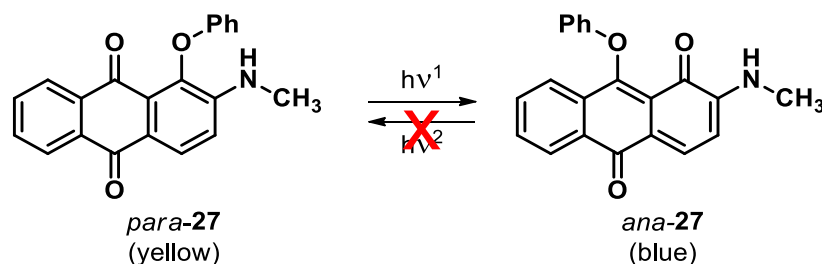
II.3. Thermal stability

Thermal stability of photoinduced isomer is one of the key parameters dictating the application area of photoswitches. It was disclosed that photogenerated *ana*-PAQs are relatively stable in the absence of irradiation. At the same time, the high moisture sensitivity of these species hampers quantification of thermal stability of *ana*-PAQs. In the first communication on the parent anthraquinone photoswitch *para*-**1**,[41] a spontaneous bleaching of *ana*-isomer in CCl$_4$ solution was detected after few days, while *ana*-**2** turned out to be more stable (Chart 5). Yokoyama and coworkers reported, that upon heating at 78 °C in toluene *ana*-**2** slowly decomposes (presumably, by the reaction with water) without formation of *para*-**2**, proving the superior thermal (but not chemical) stability of *ana*-isomer in solution.[52] Thus, the extreme sensitivity of photogenerated *ana*-isomers towards moisture should be taken into consideration upon measurement of thermal stability (for details, see Section II.6).

Chart 5. Thermal stability of some *ana*-isomers.

ana-**1**	*ana*-**2**	*ana*-**6**	*ana*-**3e**
complete back reaction:	complete back reaction:	complete back reaction:	stable at:
- 2 days in solid state	- heating at 230-240 °C	- melting at 267-268 °C	- melting at 246-247 °C
- few days in the solution	(photochromism was preserved)		

Their considerable thermal stability allowed to obtain *ana*-isomers in the crystalline state for some PAQ photoswitches (unfortunately, without X-ray crystallographic analysis), including *ana*-**2** (as orange plates),[53] *ana*-**6** (as bright orange plates),[57] *ana*-**3e** (as dark red needles).[60] For the first two photoisomers, thermal bleaching upon melting was reported. However, in the case of *ana*-**2**, the bleached sample preserved its photochromism and could be isomerized again to *ana*-**2**. The isomer *ana*-**3e** was stable upon heating (H-migration could contribute to this stability, see section II.6.1). Gerasimenko mentioned partial back reaction for a number of PAQs during recrystallization. Note, that in these cases a spontaneous interaction with moisture in the air cannot be ruled out (*vide infra*).

Quantitative evaluation of thermal stability was performed for some PAQs. Thermal stability of *ana*-**2** was estimated to be $t_{1/2} \approx 800$ d in toluene at rt ($k = 10^{-8}$ M^{-1}, $E_a = 30$ kcal/mol).[79] This value is comparable with those for thermally irreversible diarylethenes and fulgides.

At the same time, an abnormally low thermal stability of *ana*-isomers in polymeric matrix (polyvinyl acetate, polystyrene) (half-life: 0.43-17.5 h) was reported for anthraquinone derivatives *para*-**1** and *para*-**14**.[80] A possible explanation can be both the presence of moisture in the solvents used to obtain a solution of photochromic PAQ and polymer, and the moisture permeability of the polymer layer. The presence of nucleophilic impurities in PAQ-containing materials was demonstrated to be critical for the switching performance of a number of 2- and 4-acylamino-1-aryloxyanthraquinones.[81] This is also illustrated by the fact that preliminary heating of polyvinylacetate (PVA) polymer plates at 150 °C for 1 h significantly improves the thermal stability of the materials (Figure 6). The role of the preheating is to remove all water traces and decrease moisture and gas permeability of the photolayer. At the same time, storing of irradiated samples in dry atmosphere did not prevent the bleaching. Thus, the extreme water sensitivity of photogenerated *ana*-isomer requires thorough drying of the sample and protecting from moisture in the air, and such careful approach is necessary to prepare truly fatigue resistant materials.
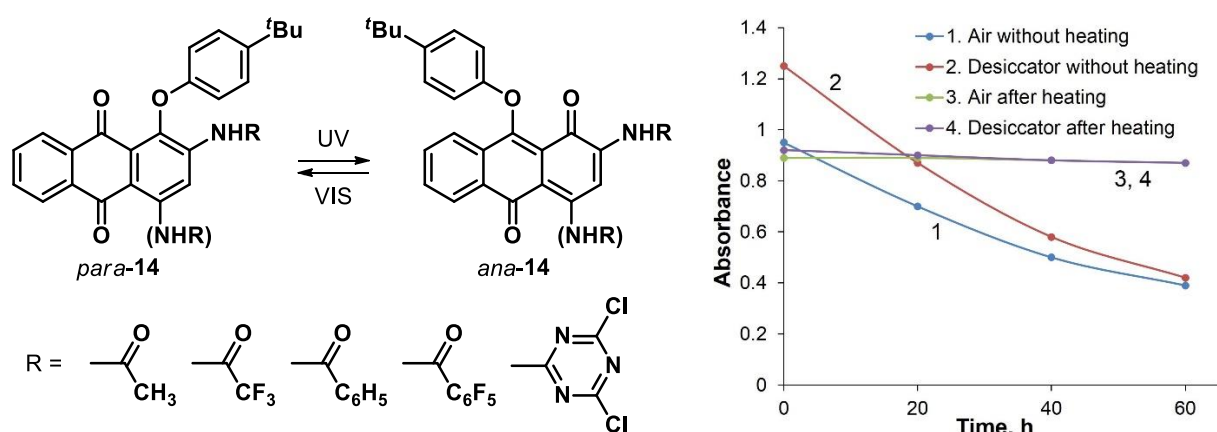

Figure 6. Photochromic performance and thermal bleaching of *ana*-isomer of PAQ **14a** in PVA matrix, dependent on prior treatment.

A boost of the thermal back isomerization by chemical stimuli has been reported for a number of photoswitches[82] and it was proposed as a way for controllable release of solar energy in molecular solar thermal (MOST) energy storage.[83] In the range of isomeric tetraethylene glycol derivatives, compounds *para*-**28b** and *para*-**28c** as well as their complexes with Ca^{2+} and Na^+ ions displayed typical PAQ photochromic performance (Scheme 8).[84] On the contrary, addition of metal ions to *ana*-**28a**, bearing a tetraethylene glycol moiety in its 8-position, resulted in spontaneous bleaching of solutions. Such destabilization of the *ana*-isomer is presumably an effect of direct coordination of the metal ion with the oxygen of the phenoxy group. Steric repulsion causes weakening of the O–Ph bond and reduces the activation energy of the back isomerization.

15

This behavior of PAQ *para*-**28a** somewhat reflects the well-known property of photochromic spiropyrans (Figure 1) to undergo ring-opening to the corresponding merocyanine in the presence of metal ions.[85]

Scheme 8. Complexation of PAQ **28a**. The X-ray structure was obtained from the Cambridge Crystallographic Data Centre via .
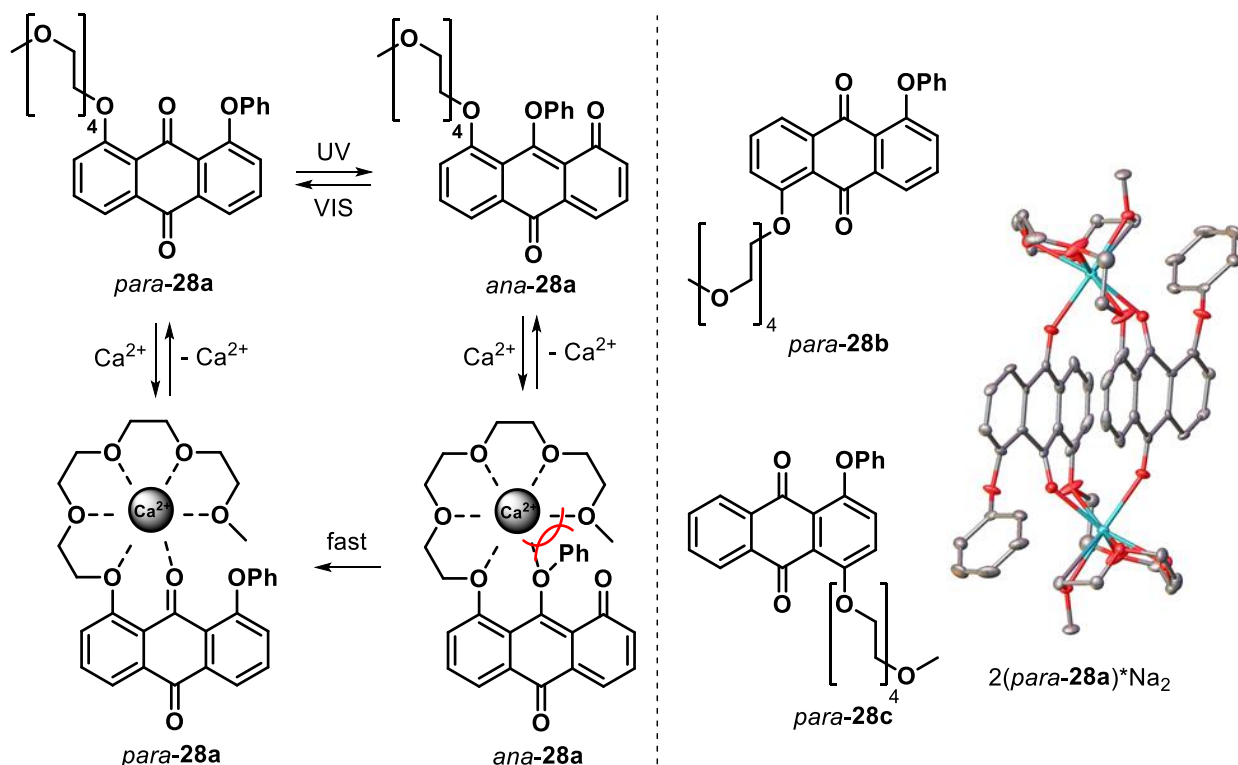
Overall, a proper determination of the thermal stability in terms of rate constant (k) or life-time ($t_{1/2}$) in solution by measurement of dark bleaching has not yet been carried out due to high sensitivity of *ana*-isomers to nucleophilic species. However, it appears to be in principle possible to perform these experiments in thoroughly dehydrated solvents.

II.4. Quantum yields

The efficiency of any photoreaction is characterized by its quantum yield and in the context of photochromism, photoswitching processes with high quantum yields require shorter irradiation times. In Table 1, values of quantum yields as reported for a number of PAQ derivatives have been collected. In general, quantum yields of direct *para*→*ana* forward (Φ_{PA}) and *ana*→*para* backward (Φ_{AP}) reactions do neither depend on the presence of oxygen[86,63] nor the nature of the solvent (acetonitrile, benzene, toluene, bromoform, cyclohexane).[63]

16

In the case of *para*-**2**, the quantum yields were measured independently by several groups. The values of Φ_{PA}, as obtained by the groups of Barachevsky[86] and Rentzepis[88] (both $\Phi = 0.60$) were sufficiently higher than estimations performed by Yokoyama and coworkers ($\Phi = 0.34$),[52] the Wirz group ($\Phi = 0.32$),[63] as well as the team of Koroteev ($\Phi = 0.30$).[87] This mismatch has been explained by incorrect determination of extinction coefficients in the case of the initial measurements and thus the lower values of the quantum yields appear correct.[63]

The influence of substituents at the migrating aryl group was probed for *para*-**2** derivatives. A reasonably high quantum yield ($\Phi_{PA} = 0.30\text{-}0.34$) was found for the unsubstituted derivative *para*-**2**. Introduction of both electron-donating and electron-withdrawing substituents to *para*-position of migrating phenyl moiety (PAQs **12a, 12d**-**j**) led to decreasing quantum yields. The strongest decrease was detected for phenylamino-substitution, i.e. PAQ **12e** ($\Phi_{PA} = 0.02$), hydroxy- and methoxy-substituted PAQs **12d** and **12j** ($\Phi_{PA} = 0.06\text{-}0.08$). The quantum yields of the backward *ana*$\rightarrow$*para* photoisomerization are several times smaller ($\Phi_{AP} = 0.015\text{-}0.10$). PAQs **12i** and **12j** carrying bromine and hydroxy substitution are an exception as the former has a forward quantum yield comparable with *para*-**2** ($\Phi_{PA} = 0.36$), whereas the latter exhibits the highest backward quantum yield ($\Phi_{AP} = 0.32$).

Table 1. Quantum yields for photochromic PAQ.

PAQ	Structure	Φ_{PA}	Φ_{AP}	Medium	Ref.
para-isomer				*ana*-isomer	
2	$R^1 = R^2 = H$	0.32	0.014	MeCN	63
		0.30	0.05	toluene	42
		0.60	-		86, 88[c]
		0.34	0.049		52
		0.30	-[a]		87
		0.36	-[a]	PMMA	87
12d	$R^1 = OMe; R^2 = H$	0.08	0.05		42
		0.07	0.035		52
12e	$R^1 = NHPh; R^2 = H$	0.02	0.015		42
12a	$R^1 = OAc; R^2 = H$	0.27	0.10	toluene	42
		0.28	0.039		52
12f	$R^1 = CN; R^2 = H$	0.26	0.075		52
12g	$R^1 = NO_2; R^2 = H$	0.20	0.05		42
		0.20	0.04		52
12h	$R^1 = C_5H_{11}; R^2 = H$	0.26	-[a]		87
		0.32	-[a]	PMMA	87
12i	$R^1 = Br; R^2 = H$	0.36	0.10	toluene	43

17

12j	R^1 = OH; R^2 = H	0.06	0.32	toluene	43
3e	R^1 = H; R^2 = NH$_2$	0.02	0.007	toluene	54
3f	R^1 = H; R^2 = NHC(O)Ph	0.09	0.016	toluene	54
		0.08	-[a]	toluene	87
		0.19	-[a]	PMMA	87
3g	R^1 = H; R^2 = NMeAc	0.09	0.005	toluene	54
		0.016	-[a]	toluene	87
		0.021	-[a]	PMMA	87
3h	R^1 = H; R^2 = NHPh	0.0008	-[b]	toluene	54
3i	R^1 = H; R^2 = NHC(O)CH$_2$Cl	0.19	0.1	toluene	54

5	Het = (pyridine)	0.20	0.07	toluene	54
7a	Het = (pyrrole–Ph)	0.22	0.015	benzene	55

29	-	0.27	0.08	toluene	54

[a] Quantum yields have not been measured; [b] No photoisomerization was detected; [c] In benzene.

Introduction of amino groups in the 6-position of *para*-**2** results in PAQ derivatives *para*-**3e,f-h** that show a significant decrease of their quantum yields, partly due to competing side reactions.[54] An exception is PAQ *para*-**3i**, where the amine was substituted by a strong electron-withdrawing group. Replacement of the benzene by a pyridine or pyrrole ring yielding PAQ derivatives *para*-**5**[54] and *para*-**7a**,[55] respectively, as well as *peri*-annulation by a pyridone ring leading to PAQ *para*-**29**[54] reduce the efficiency of the forward photoreaction while practically not affecting the backward reaction.

A comparison of direct quantum yields for a number of substituted aryloxynaphthacenequinones in toluene and various polymeric matrices (polymethyl methacrylate (PMMA), polyvinyl butyrate, and polybutyl methacrylate) was performed.[87] It turned out that the quantum yields of photoisomerization in polymer films are higher than in toluene for all studied compounds and polymers. For example, the quantum yields of direct isomerization of PAQ *para*-**3f** were found to be more than twice as high in a PMMA matrix as compared to solution.

The effect of substitution at the migrating group on photoreactivity is somewhat different in the series of aryloxy-substituted benzo[*h*]naphtho[1,2,3-*de*]chromene-2,8-diones **8** (Figure 7).[89] In this case, strong electron-donating (OMe) and electron-withdrawing (NO$_2$) substituents greatly

18

slow down the photoisomerization process. Since the spectral properties are barely affected, this indicates significantly lower quantum yields. However, in addition, it can be assumed that the longer time to reach PSS may be due to increased sensitivity of the formed *ana*-isomers **8d** and **8e** to impurities in DMSO, e.g., water.
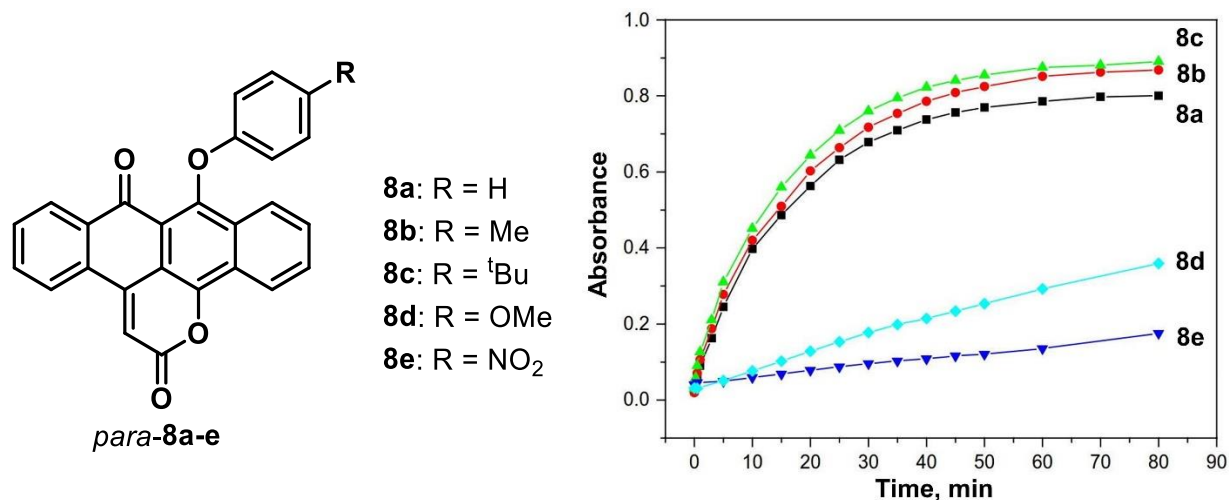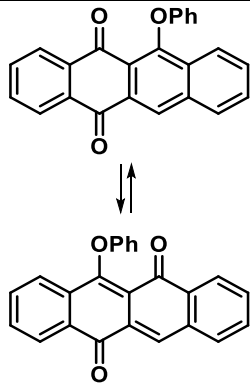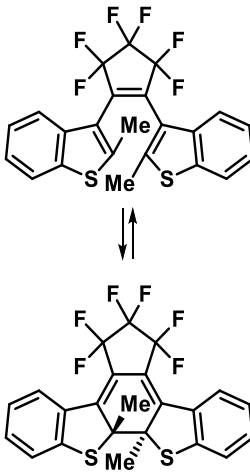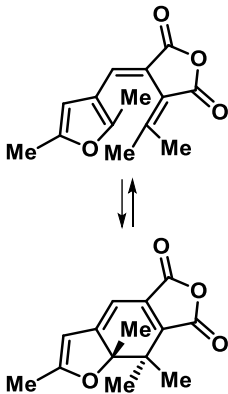

Figure 7. Change of absorbance in the maximum of *ana*-isomer upon irradiation with UV (365 nm) in DMSO for PAQs **8**. Adapted with permission from ref. [89]. Copyright 2011 Elsevier.

In attempt to benchmark the PAQ system, we performed a comparison of the photochromic properties of *para*-**2** with selected examples of thermally stable photoswitches, i.e., diarylethene **DAE** and fulgide **FF** (Table 2). The first one was reported by Irie and coworkers[90] and has become one of the most successful diarylethene derivatives due to its excellent thermal stability and fatigue resistance. The fulgide **FF** was described by Heller and Langan[91] and has been used as a chemical actinometer due to its superior performance (commercially sold as Aberchrome 540). In comparison with these examples, *para*-**2** possesses a noticeably red-shifted absorbance. Extinction coefficients of the three types of photoswitches are comparable due to similar shift from the more aromatic isomer in the resting state to the less aromatic photogenerated isomer with a conjugated π-system. Quantum yields of the forward isomerization are somewhat comparable for all compounds, while the quantum yield of the backward reaction for *para*-**2** is low similarly to **FF** and most diarylethenes (note that the referenced **DAE** is a rare example of a diarylethene with high cycloreversion efficiency). Thus, the photochromic characteristics of PAQ photoswitches are similar to those of other well-studied classes of thermally irreversible photoswitches, namely diarylethenes and fulgides.

19

Table 2. Comparison of spectral properties and quantum yields of *para*-**2** with selected examples of other photochromic families.

№	Photochromic performance	Solvent	λ_A^{max}, nm (ε, M^{-1}cm^{-1})[a]	λ_B^{max}, nm (ε, M^{-1}cm^{-1})[b]	Φ_{AB}[c]	Φ_{BA}[d]	Ref.
para-**2**		MeCN	390 (5500)[e]	470 (12000)[e]	0.32	0.014	63
DAE		MeCN	257	525	0.27	0.22	92
		Hexane	298 (6800)	515 (10000)	0.31	0.32	93
FF		EtOAc	340 (6270)	492 (8850)	0.18	0.06	94

[a] Absorption maximum (extinction coefficient) of ground-state isomer **A**
[b] Absorption maximum (extinction coefficient) of photogenerated isomer **B**
[c] Quantum yield of the direct photoisomerization
[d] Quantum yield of the back photoisomerization
[e] Approximate values, obtained by analysis of the reported spectra [ref. 63]

II.5. Fatigue resistance

In a number of studies, a high fatigue resistance of naphthacenequinone-based PAQs up to 500 cycles was mentioned.[95] Multiple switching was reported for PAQ-derived materials (see Section IV.4). As an example, repetitive photoswitching of a selected PAQ **14a** in dichloromethane is

20

shown in Figure 8.[62] The initial solution of the *para*-isomer absorbs at 380 nm yet an insignificant fraction of the *ana*-isomer (λ^{max} = 545 nm) was also observed due to impact of ambient light. UV irradiation results in the growing of the absorbance in the visible region. After reaching the PSS composed of 82% *ana*-isomer (based on ^{1}H NMR spectroscopy), the solution was irradiated with green light resulting in almost complete recovery of the initial spectrum. After five such cycles of forward and backward photoswitching, a decrease of absorbance at 545 nm by ca. 10% was observed. This degradation is once again most likely due to an unwanted reaction of the sensitive *ana*-isomer with ambient moisture.
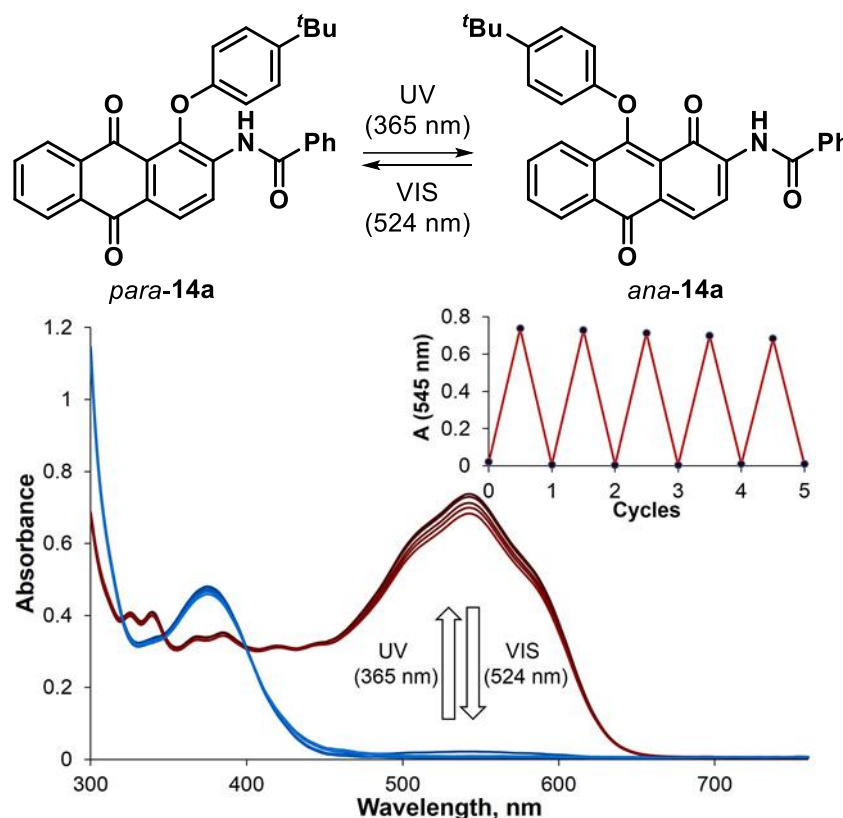
Figure 8. Photochromic performance and fatigue resistance of PAQ *para*-**14a**.

The main fatigue reaction of PAQs is interaction with water (for details, see Section II.6.). Rentzepis and coworkers disclosed another fatigue mechanism, connected with the participation of highly reactive triplet species in the photoswitching mechanism (Scheme 10).[88] It was proposed, that hydrogen abstraction could compete with the last step of photoswitching process, consisting of intersystem crossing from the triplet state of *ana*-**PQ** to its corresponding singlet ground state. In the presence of isopropanol, the quantum yield of the forward photoreaction of *para*-**2** decreased and the quantum yield of irreversible photodegradation of *ana*-**2** increased. Both findings corroborate irreversible photodecomposition caused by triplet-state H-abstraction.

21

Scheme 10. Decomposition pathway of PAQs.

$$\textit{para-}\textbf{AQ} \xrightarrow{h\nu} \cdots \longrightarrow T_1 (\textit{ana-}\textbf{AQ}) \longrightarrow \textit{ana-}\textbf{AQ}$$

$$\downarrow \textit{i-}\text{PrOH}$$

$$[\textit{ana-}\textbf{AQ}]H^{\bullet} \longrightarrow \text{decomposition}$$
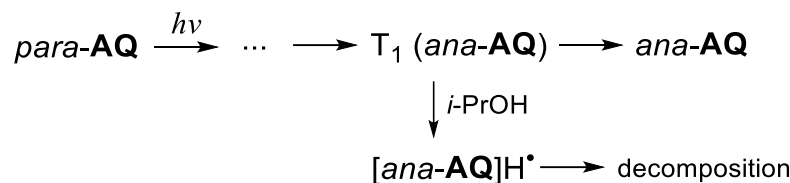
Thus, up to date two pathways of fatigue of PAQs have been disclosed. The first one is connected with thermal (ground-state) reactions of *ana*-isomers, while the second one is a result of the high reactivity of a transient triplet species. From this insight it appears that a proper choice of the reaction medium (removal of water and other nucleophilic impurities, such as alcohols and amines, and absence of good H-atom donors) is a way to get around these obstacles.

II.6. Reactivity of *ana*-isomers

A somewhat undesired and at the same time unique feature of PAQ photoswitches is a pronounced sensitivity of photogenerated *ana*-isomers to nucleophiles. For the first time, this property was reported by Gerasimenko and coworkers.[40] They found, that irradiation of *para*-**1** in alcohols as solvents did not result in colored species. In addition, continuous irradiation of benzene solution of *para*-**1** resulted in quantitative conversion to 1-hydroxyanthraquinone **30a** (Scheme 11A). A notable sensitivity of the *ana*-isomers to nucleophilic species in the solution is in the heart of these findings. Amines were considered as convenient reagents to study the origin of such an activity. Gerasimenko and his team failed to obtain the products of the interaction of *ana*-**1** with amines due to the extreme water sensitivity. Naphthacenequinone derivative *para*-**2** was found to be more suitable for the reaction with ammonia and aniline. Irradiation with subsequent treatment with primary amines resulted in a quantitative formation of adducts **31a** (Scheme 11B).[53] Initial *para*-isomers do not react with amine, and such a reactivity is an intrinsic property of the *ana*-isomers.

Scheme 11. Reactions of *ana*-PAQs with nucleophilic species.

22
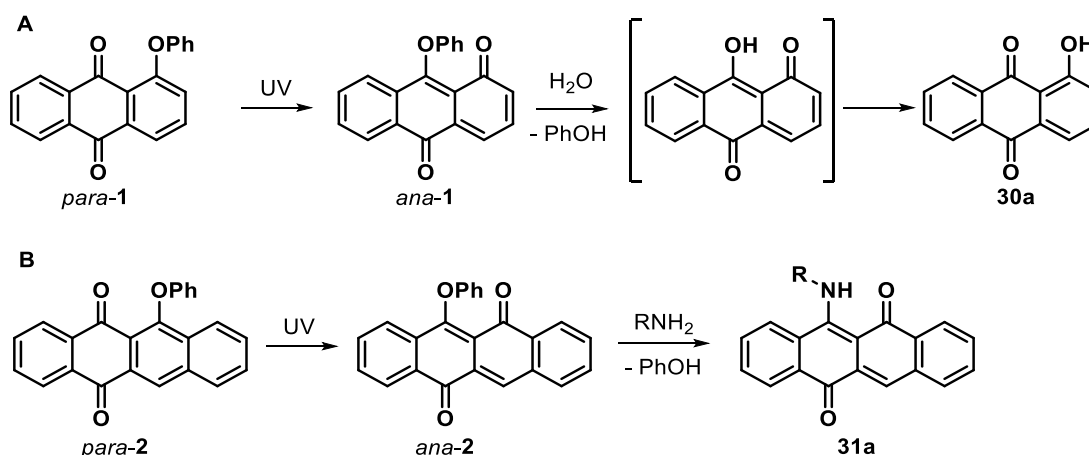
The primary stage of the reaction between *ana*-PAQ and nucleophiles (water, alcohols, primary amines) is nucleophilic conjugate 1,4-addition. According to calculations, this process is the exergonic one.[96] The selectivity of the nucleophilic attack at position 4 (Scheme 12) may be rationalized in terms of the charge distribution[97] or the largest coefficient in the LUMO of the *ana*-PAQ molecule.[98] The next step of the reaction, i.e., phenol (ArOH) elimination, is strongly dictated by the structure of the primary adduct.[96,99] The adducts with water **32** are unstable (but could be detected spectroscopically) and spontaneously eliminate a phenol and form stable *peri*-hydroxyanthraquinones **30** (Scheme 12A). For adducts with alcohols **33** (Scheme 12B), this elimination is endergonic and can be realized thermally or photochemically. After elimination of phenol, the second alcohol molecule can add to intermediate **34** and form acetals **35**. Depending on the reaction time, intermediates **33** and **35** could be isolated in case of anthraquinone PAQs.[97]

Scheme 12. Reactions of *ana*-PAQs with nucleophiles: water (A), alcohols (B), amines (C).
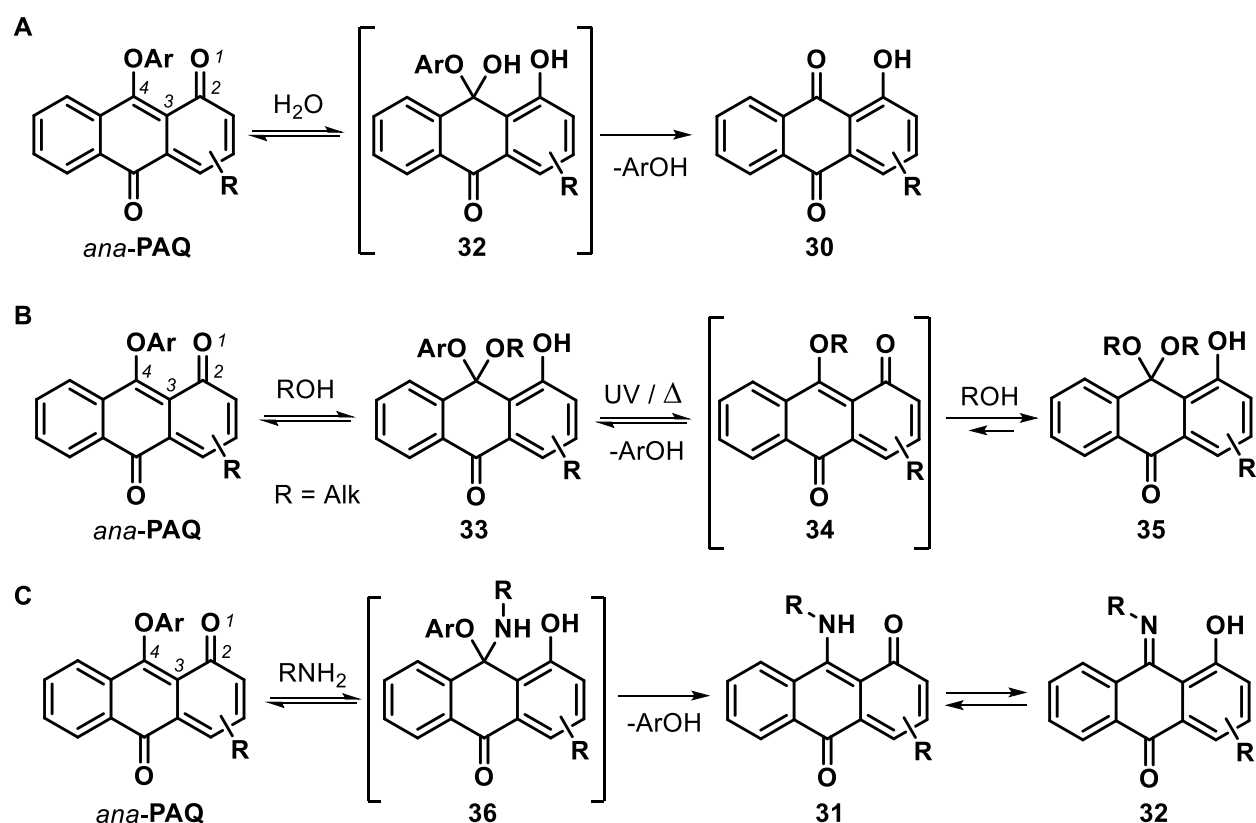
On contrary, the primary adducts of *ana*-PAQ with primary aliphatic and aromatic amines **36** are thermodynamically unstable and spontaneously eliminate phenol (Scheme 12C). The resulting species exists as a mixture of two tautomeric forms: enaminoquinoid **31** and oxy-imine **32**. Their interconversion can conveniently be controlled by solvent polarity (Table 3).[99] In hexane,

23

the equilibrium is shifted almost exclusively to the oxy-imine (96%) while the content of the enaminoquinoid increases up to 41% in ethanol. Secondary amines such as piperidine did not form corresponding adducts with *ana*-isomers, however, they boost the hydrolysis of *ana*-isomers by water.[60,77]

Table 3. The content of equilibrium mixture **31b**/**32b** in various solvents (left). Example of absorbance changes for **31b**/**32b** analogue in EtOH, CHCl$_3$, and hexane (right).

Solvent	**31b** (in %)	K_{eq}
Hexane	4.0 ± 0.5	24 ± 3
CCl$_4$	5.4 ± 0.7	17 ± 2
Ethyl acetate	8.3 ± 1.0	11 ± 1
CH$_2$Cl$_2$	16 ± 2	5.3 ± 0.8
Acetonitrile	18 ± 2	4.6 ± 0.6
CHCl$_3$	20 ± 3	4.0 ± 0.7
Isopropanol	30 ± 4	2.3 ± 0.4
Ethanol	41 ± 5	1.4 ± 0.2

As expected, the nature of nucleophiles largely affects the rate constant (*k*) of conjugate 1,4-addition. Therefore, the rate constant is decreased by about four orders of the magnitude upon transition from alkyl amines to alcohols.[96] Rate constants of 1,4-addition employing aromatic amines perfectly correlate with Hammett constants for various electron-donating and electron-withdrawing groups and the resulting linear energy free relationship indicates one and the same mechanism across the entire substrate spectrum.[98]

Quantitative evaluation of reactions with nucleophiles was performed for some PAQs (Table 4).[96] According to this study, naphthacenequinone derivative *ana*-**2** is significantly less reactive towards methanol than *ana*-anthraquinones (compare entries 7 and 1,3,5,6 in Table 4). Even the most stable 2-aminosubstituted 9-phenoxy-1,10-anthraquinone has an about one order of magnitude higher value of the rate constant for the reaction with methanol. Kinetic analysis with *iso*-propylamine clearly demonstrates that the photogenerated form of phenoxy-quinones can largely be stabilized by introducing donor substituents in the quinone rings.

24

Table 4. Reaction rate constants of photogenerated *ana*-isomers with methanol (k_1), water (k_2), and *iso*-propylamine (k_3) in toluene at 298 K.

entry	№	Structure	Rate constants		
			CH$_3$OH	H$_2$O	^{i}PrNH$_2$
			k_1, M^{-1}c^{-1}	k_2, M^{-1}c^{-1}	k_3, M^{-1}c^{-1}
1	*ana*-**37a**		4.2	-	$2.1 \cdot 10^4$
2	*ana*-**37b**		-	-	$5.8 \cdot 10^3$
3	*ana*-**1**		0.3	0.02	150
4	*ana*-**37c**		-	-	21
5	*ana*-**37d**		$7 \cdot 10^{-3}$	-	5.4
6	*ana*-**27**		$3 \cdot 10^{-4}$	-	4
7	*ana*-**2**		$\approx 10^{-5}$	-	

Usually, *ana*-isomers of PAQs are unstable in ethanol solutions. Thus, in 96% solutions of ethanol, the rate constants for the nucleophilic addition of *ana*-**2** and *ana*-**7a** were 1.1×10^{-4} s^{-1} and 7.6×10^{-5} s^{-1}, respectively (Figure 9A).[55] These values correspond to half-lives as high as 1.8 h and 2.5 h, respectively. Moreover, an unexpected stability of some heteroannulated PAQ analogues was reported. PAQs **10**,[59] **38**,[59] and **39**[66] were switchable even in the alcohol solutions (Figure 9B). Surprisingly, photogenerated *ana*-**10** was more stable in ethanol than in toluene upon irradiation. Probably, the presence of the electron-donating amino group (as part of the pyridone) in the quinone π-system contributes to this phenomenon.

A. Half-lifes for ana-isomers in 96% ethanol solutions

ana-**2**
($t_{1/2}$ = 1.8 h)

ana-**7a**
($t_{1/2}$ = 2.5 h)

B. PAQs, switchable in ethanol solutions

10

38

39

1 – Before irradiation
2 – After UV irradiation
3 – After VIS (> 460 nm)
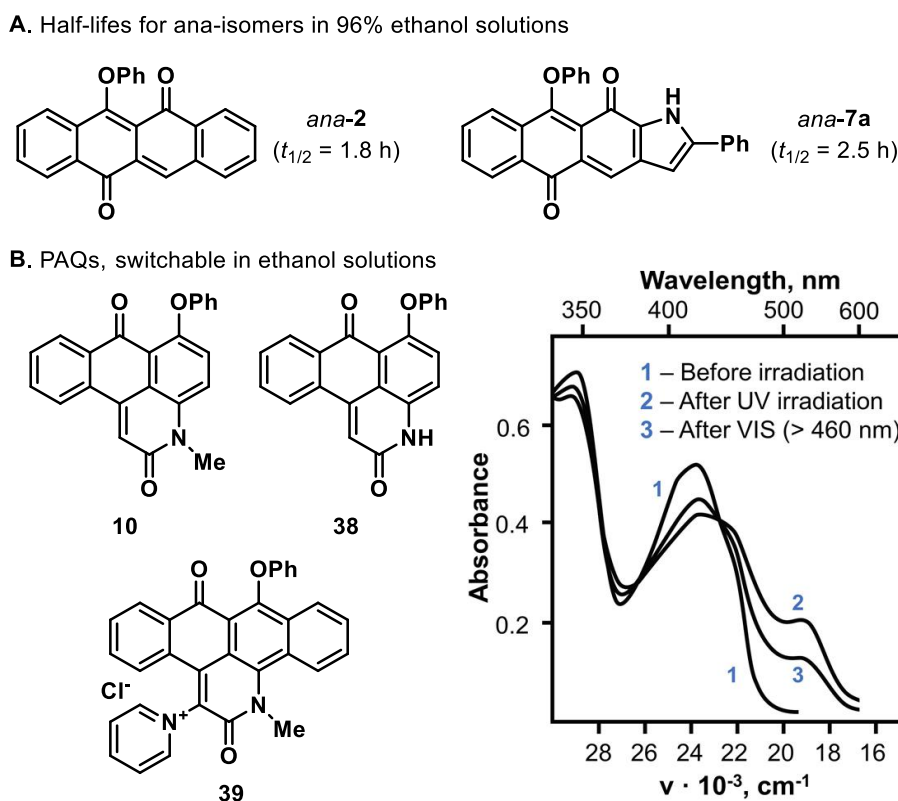
Figure 9. Stability of *ana*-isomers in ethanol solutions (A). PAQs, switchable in ethanol solutions (B, left). Spectral changes of **10** in ethanol upon irradiation with different wavelengths (B, right).

The pathway of the reaction of *ana*-isomers with nucleophiles strongly depends on minor changes in the structure. While *ana*-**2** readily reacts with aniline (isolated yield 40% after 0.5 h,[53] Scheme 9), its analog **12d** with a 4-methoxy group in the migrating aryl group does not react with aniline.[100] At the same time, 9-phenoxy-1,10-anthraquinone *ana*-**1** readily reacts with aniline.[98]

Some more complicated reactions with amines were found for *ana*-isomers of 4-methoxy-substituted anthraquinone **37d** (Scheme 13).[78] Reaction with ammonia led mainly to the substitution of the OMe group and formation of **41**, consisting mainly in the imine tautomer of 1,4-quinone **42**. The last species are extremely stable towards nucleophiles as demonstrated by the fact that they are soluble in alkaline solution (for further details see the next section).

Scheme 13. Reaction of *ana*-**37d** with ammonia.

ana-**37d** → **40** (minor) + **41** (major) ⇌ **42**

26
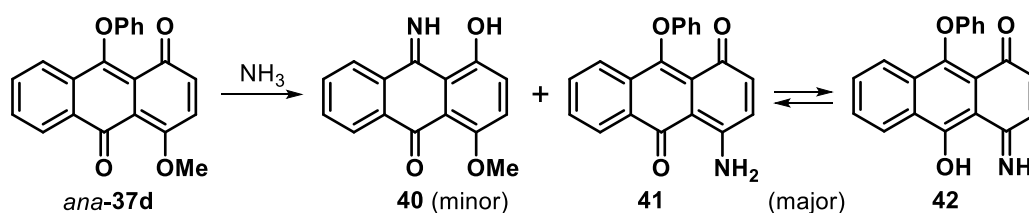
II.6.1. Stabilization of photoisomers by additional migrations

Photogenerated isomers of certain PAQs can significantly be stabilized by an additional step of either hydrogen or acyl migration. After photolysis of independently synthesized 4-amine-1-phenoxyanthraquinone *para*-**37e** (Scheme 14A, compare with Scheme 13), its corresponding photoisomer **44**, obtained as a result of H-migration in the *ana*-isomer, was isolated in the crystalline state.[74] This compound was stable even in aqueous potassium hydroxide solution. The drawback of this photoswitch is a low PSS conversion (only up to 20%), probably due to pronounced photoinduced charge transfer process.

Scheme 14. Photoisomerization / migration reactions for PAQs.
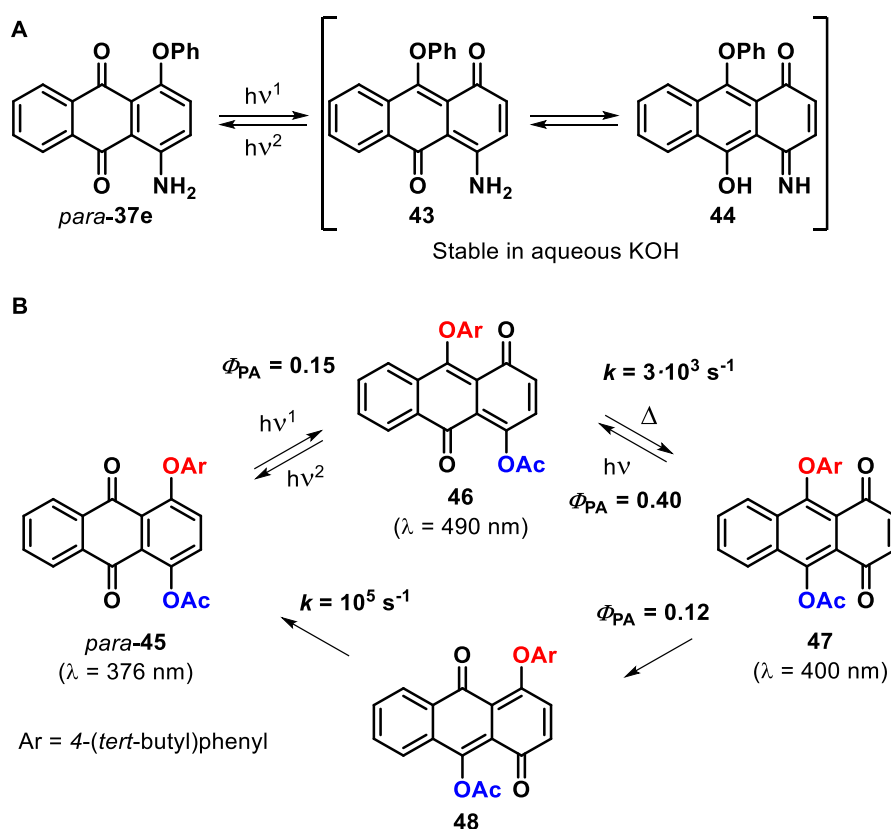
4-Hydroxy- and 4-acetyloxy-substituted anthraquinone PAQs also participate in tandem post-irradiation processes (Scheme 14B).[78] A mechanistic study was performed for *para*-**45**.[101] Upon irradiation at room temperature, *para*-**45** formed a stable photoproduct with slightly shifted absorbance maximum at 400 nm corresponding to the structure of 1,4-benzoquinone **47**. At 77 K it was possible to detect two intermediates **46** and **48**. The first one, **46**, was formed by aryl group migration from *para*-**45**. For this species, a fast acyl migration was detected towards **47**. Upon irradiation, **47** was involved in two processes: back acyl migration towards **46** (Φ_{PA} = 0.40) and

27

aryl group migration towards **48** ($\Phi_{PA} = 0.12$). *Ana*-quinone **48** is thermally unstable and undergoes a fast isomerization to *para*-**45**. Thus, the direct and back reactions of *para*-**45** proceed *via* different pathways.

II.6.2. Anomalous photoproducts

The pronounced chemical activity of the *ana*-isomers in some cases causes an unexpected behavior of photogenerated species. Pyrazoloanthrone-based PAQ *para*-**21** bearing a phenoxy group in its 5-position shows photochromism with an expected photoinduced maximum at 440 nm (Figure 10A,B).[69] However, its analog *para*-**49** with a phenoxy group in 7-position upon light irradiation forms photoinduced species with extremely red-shifted and broad maxima up to 577 nm (Figure 10C,D). These species were thermally and photochemically unstable and formed *ana*-**49**, which was subjected to reactions with water and butylamine with formation of corresponding adducts. Zwitterionic *spiro*-intermediate **50** was proposed to be the observed species, possibly stabilized by charge delocalization in the pyrazole fragment and aromatization of the anthracene core.
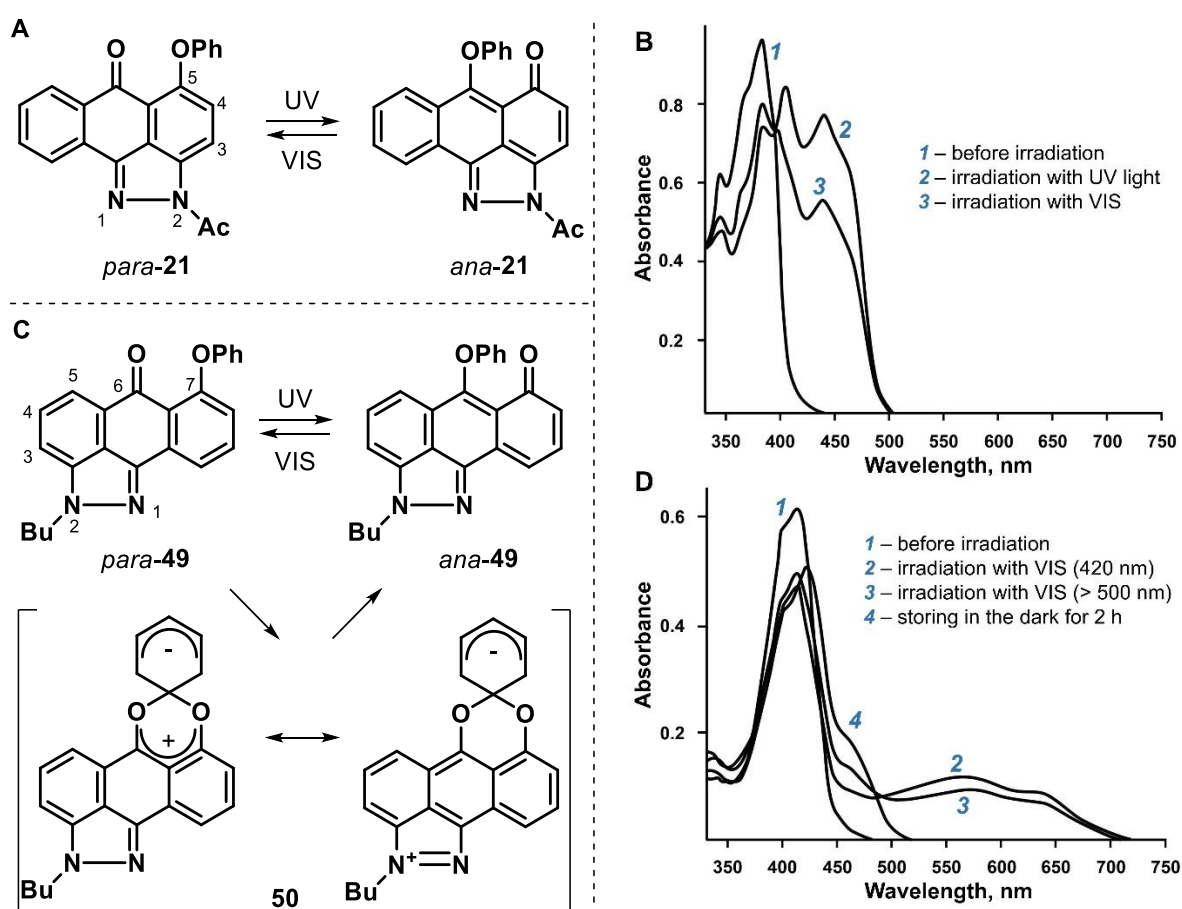
Figure 10. Proposed photochromic performance and spectral changes in toluene of PAQs **21** (A and B, respectively) and **49** (C and D, respectively).

28

II.5. Switching in the solid state

In this section we present the results of PAQ photoswitching in various solids of increasing order from polymers over 2D-assemblies to crystals.

Blended and functionalized polymer thin films. In early works, photochromic thin film materials were prepared by blending of PAQs with polymers. Polyvinyl acetate and polystyrene were prepared with 2-22% content of PAQs with < 80 μm thickness.[80] PMMA, polyvinyl butyral, as well as polybutyl methacrylate have been used for preparation of materials with 10-15 wt% PAQ content and 2-3 μm thickness.[87]

Three types of macromolecular photoswitches with covalently-bonded PAQs were prepared by functionalization of poly(methyl methacrylate) (PMMA), polystyrene, and polysiloxane bearing active ester pendant groups (Figure 11).[95] PAQ **51** containing an amino group was successfully connected via amide linkages by replacing the N-hydroxysuccinimide active ester moieties to achieve functionalization of 90% PAQ on the polymer backbone.
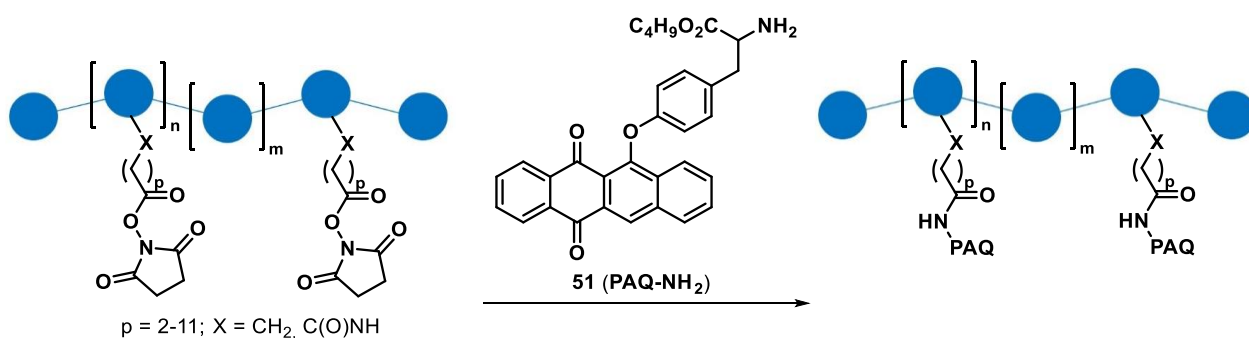
Figure 11. Post-modification of polymers by PAQ **51**.

All polymers obtained were photoactive.[64] Shifting from the single-molecule level in solution across polymer solution to the corresponding thin films results in gradual decreasing of direct quantum yield (Φ_{PA}) probably due to the increasing viscosity. For **51**, **51**-based polysiloxane in ether, and a **51**-based film (X = CH$_2$, p = 9), the initial rates of *ana*-product formation dropped in the order of 100, 66, and 44. Photoswitching is affected by the length of the linker between the main chain and the PAQ group, concentration of the PAQ groups, and the type of the polymer backbone as well as the sidechains. Interestingly, elongation of the alkyl linkers in the sidechain of polysiloxane (from p = 2 to p = 9) led to a decrease of the initial rate of *ana*-product formation. In general, it appears that thin films with a high PAQ content can be prepared while retaining their photochromic and mechanic properties.

Various polymerization methods have been applied for PAQ derivatives (Chart 7). PAQs with pendant vinyl and methacrylate groups undergo AIBN-initiated radical copolymerization
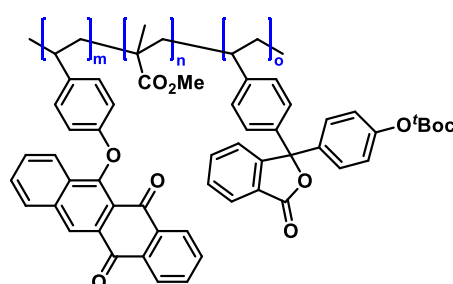
29

with styrene[102,103] (**52**, **55**) and methyl methacrylate (**53**, **54**).[103,104] Pd-catalyzed addition copolymerization towards **56** and **57** with $\{(\eta^3\text{-allyl})Pd\text{-}(SbF_6)\}$ as the catalyst was reported for norbornene-based monomers.[105] Ring-opening metathesis polymerization (ROMP) in the presence of first generation Grubbs catalyst was successfully applied for synthesis of copolymers **58** with porphyrin derivatives.[106] The obtained materials were photoactive in all cases.
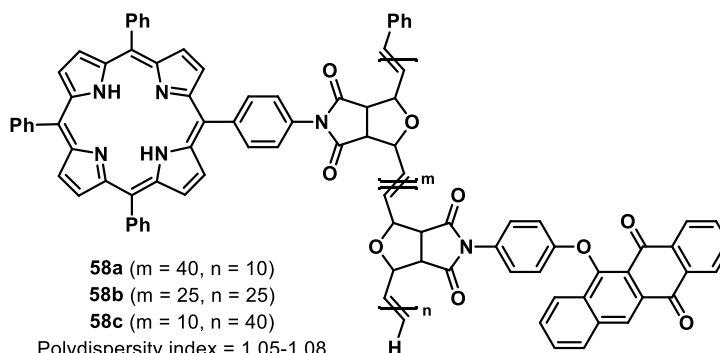
Chart 7. Photochromic PAQ-based polymers.

Switching in self-assembled thin films. Two-dimensional assemblies of photochromic molecules on surfaces, including liquid/solid interfaces, have been prepared and investigated during the last decades.[107] Langmuir–Blodgett (LB) technology was used to prepare stable and ordered structures comprising from 1 to 40 monolayers of PAQ **2** on highly oriented pyrolytic graphite (HOPG).[108,109] These multilayer assemblies with ultrahigh PAQ density were shown to be photoactive and scanning tunneling microscopy (STM) allowed monitoring of the photochromic reaction from

30

para-**2** to *ana*-**2**. As can be seen from Figure 12, STM current images of the LB layer are noticeably different for *para*- and *ana*-isomers reflected in the significantly altered packing parameters.
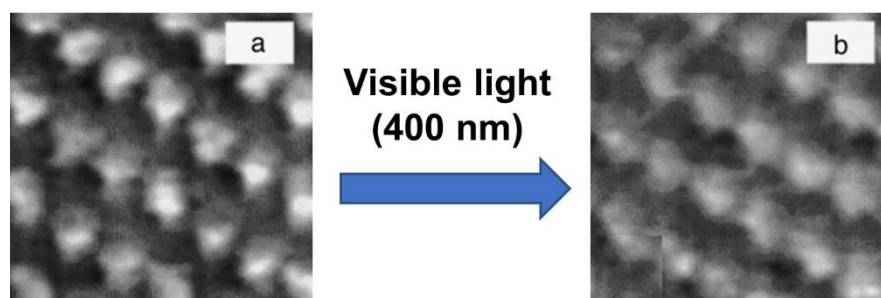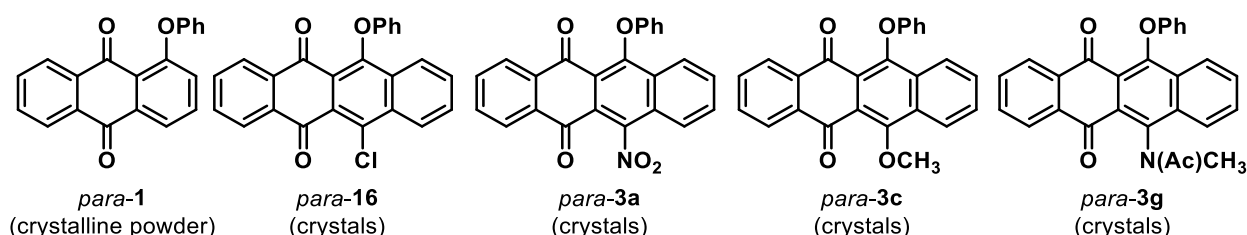

Figure 12. STM current images of 3-layer PAQ **2** Langmuir–Blodgett films before (a) and after irradiation (size *ca.* 2.2 nm × 2.2 nm). Adapted with permission from ref. [108]. Copyright 2000 Elsevier.

Crystalline state. Gerasimenko and coworkers briefly reported the photoactivity for a number of PAQs crystals (Chart 8). Yellow crystals of the presented compounds become orange or reddish orange upon exposure to sunlight or UV light.[40,60] Unfortunately, no further information regarding this phenomenon has been reported. The extent of light penetration into bulk crystals depends mainly on extinction coefficients and this value can reach up to millimeters in the case of some diarylethenes.[14] Therefore, it would indeed be interesting to investigate the photoswitching of PAQ crystals and compare them with diarylethenes.

Chart 8. PAQs that display photoswitching in the crystalline state.

para-**1**
(crystalline powder)

para-**16**
(crystals)

para-**3a**
(crystals)

para-**3c**
(crystals)

para-**3g**
(crystals)

II.7. Electronic structure and redox properties

Frontier molecular orbitals of *para-* and *ana-***4** were computationally studied by Jacquemin and coworkers (Figure 13).[110] In the case of *para-***2**, electron density in the HOMO is substantially located on the migrating phenyl group. The calculations suggest that electronic excitation is associated with partial electron transfer from the phenyl moiety to the anthraquinone core. In the corresponding *ana-*isomer, on the contrary, the phenyl ring plays a negligible role and both the HOMO and the LUMO are delocalized over the entire quinone core.
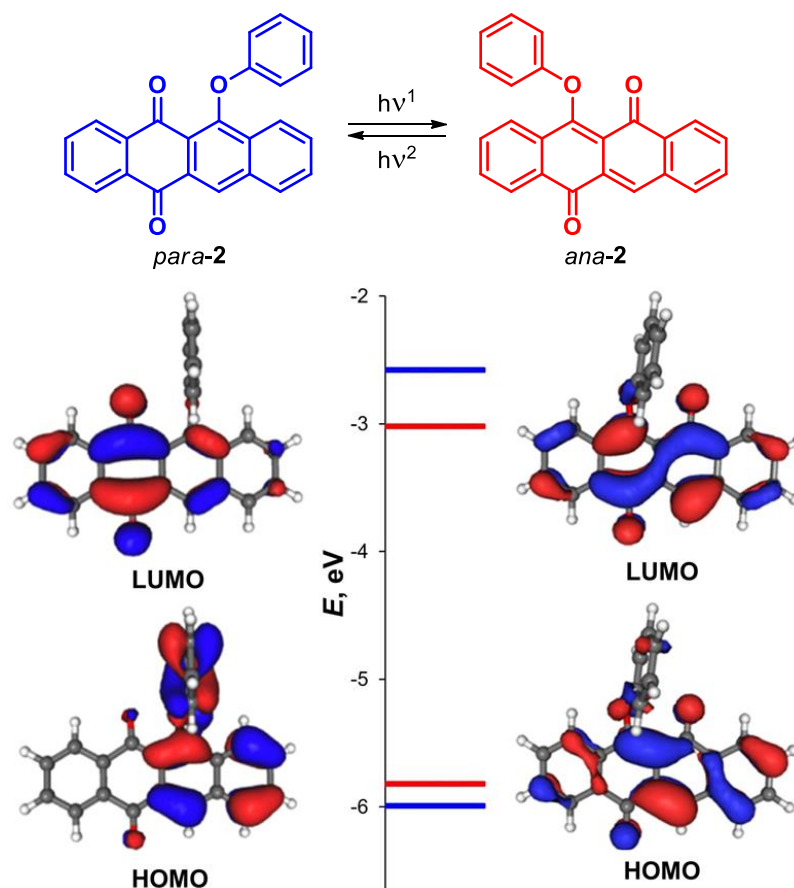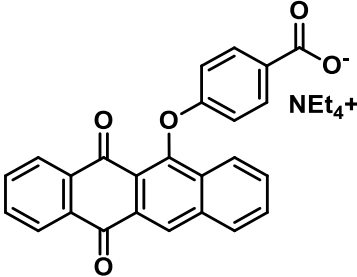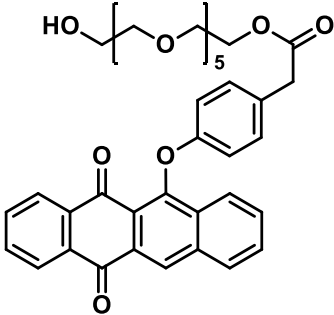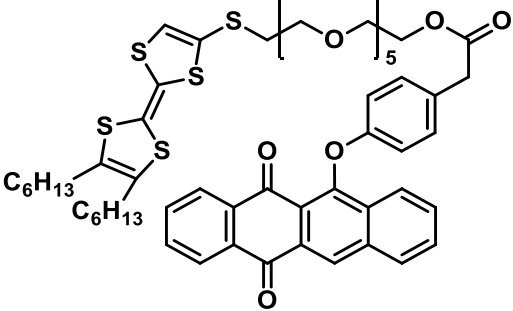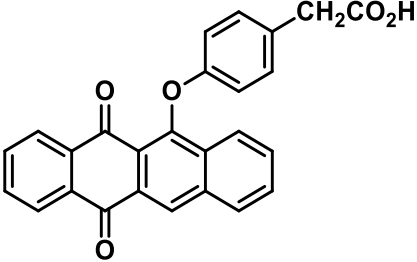

Figure 13. Frontier molecular orbitals for PAQ **2**. Adapted with permission from ref. [110]. Copyright 2011 Elsevier.

The redox properties for a number of PAQs were studied by cyclic voltammetry (Table 5). Structurally resembling quinones, these compounds are good acceptors of electrons. Branda and coworkers described the reduction process of naphthacenequinone derivative *para-***59** (Figure 14).[111] In line with the computational data above predicting a lower LUMO level for the *ana-*isomer, it was indeed shown that *ana-***59** with a cathodic peak potential of $E_p^c = -0.72$ V acts as a better electron acceptor than the *para-*isomer *para-***59** ($E_p^c = -1.15$ V). Reduction potentials were also measured for PAQs *para-***60** and *para-***61**.[112] For both compounds a significant increase of the

reduction potentials was reported upon *para*-to-*ana*-photoisomerization was reported. This has been further confirmed by theoretical calculations predicting the LUMO energy of *ana*-**60** (E_{LUMO} = -3.02 eV) to be lower than the one of the corresponding *para*-**60** (E_{LUMO} = -2.58 eV). Moreover, the reduction potentials for PAQ *para*-**62** were also reported.[61]

Table 5. Redox properties of some PAQs.

PAQ	Structure	Isomer	Cathodic peak potential $E_{\mathrm{p}}^{\mathrm{c}}$, V
para-**59**		*para*-	-1.15[a]
		ana-	-0.72[a]
para-**60**		*ana*-	-0.61[b]
para-**61**		*para*-	< -0.8[b]
		ana-	-0.74[b]
para-**62**		*para*-	-0.91, -1.46[c]

[a] Fc/Fc⁺ electrode as the reference electrode. [b] Ag/Ag⁺ electrode as the reference electrode.
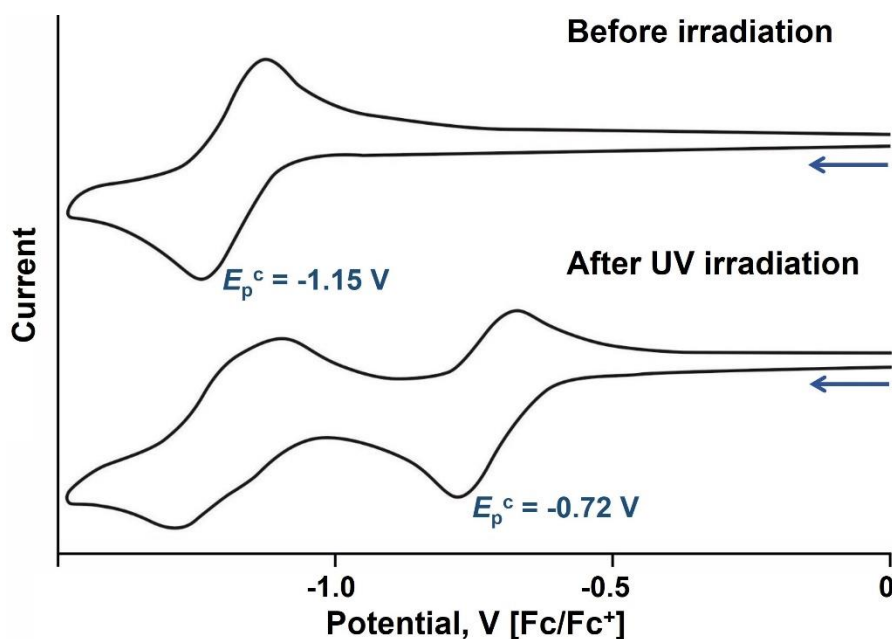[c] Saturated calomel electrode (SCE) as the reference electrode.

Figure 14. Cyclic voltammograms (showing reduction processes) of CH_2Cl_2 solutions of PAQ *para*-**59** (*vide infra*) and the photostationary state upon irradiation with 365 nm light (bottom). Adapted with permission from ref. [111]. Copyright 2001 American Chemical Society.

Manipulation of charge transport through single photoswitch molecules is of fundamental interest for molecular electronics. In this context, the photoresponsive molecule should possess a bistability as well as significant differences in the electronic structure of both isomers, enabling high and low conductance states. Diarylethenes satisfy these requirements and thus have been extensively studied in this direction.[113,114] PAQ switches could also be considered for such applications. While in the *para*-isomer, there are two isolated π-systems that are separated by a benzoquinone unit, in the *ana*-isomer, π-conjugation extends over the entire molecule. Thus, the *ana*-isomers are expected to exhibit higher conductance when compared to the *para*-isomers. Indeed, PAQ photoswitches have been studied in this context – at least *in silico* – in a number of papers[115,116] and these theoretical results reveal the potential of PAQs for molecular electronics applications.

II.8. Switching by chemical stimuli

PAQs can be switched not only by light but also by chemical stimuli. 6-Substituted 11-phenoxy-naphthacene-5,12-quinones can be converted to *ana*-isomers by addition of Lewis or Brønsted acids (Scheme 18).[117] In the case of 6-amino-substituted derivatives, the major component of the equilibrium mixture is the *ana*-isomer, while in other cases the equilibrium is shifted towards the *para*-isomer. Thus, treatment of *para*-**3e** by sulfuric acid resulted in an equilibrium mixture containing 11% of *para*-isomer and 67% of *ana*-isomer. The same mixture was obtained after acid

34

treatment of the *ana*-isomer, proving equilibration. Interaction of *para*-**3e** with aluminum chloride resulted in mixture of 76% of the *para*-isomer and 22% of the *ana*-somer. Treatment of *ana*-**3e** leads to mixture with 4% of *para*-isomer and 92% of *ana*-isomer. Analogues of *para*-**3e** bearing various substituents instead of the amino-group (H, OMe, OPh) also undergo this transformation. Such bidirectional switching using distinct chemical stimuli are reminiscent the dihydroazulene-vinylheptafulvene class of photochromic molecules (Scheme 18).[118] Direct cycloreversion of 1,1-dicyanodihydroazulene can be induced photochemically or alternatively by addition of a strong Lewis acid such as AlCl$_3$. The back reaction from the thus formed vinylheptafulvene can be performed thermally as well as by addition of mild Lewis acids that significantly boost cyclization.

Scheme 18. Chemical switching of PAQs in analogy to dihydroazulene-vinylheptafulvene switches.

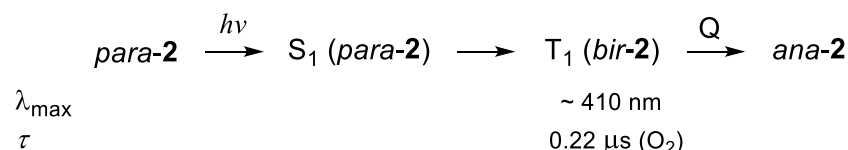Dihydroazulene (DHA) / vinylheptafulvene (VHF) switching
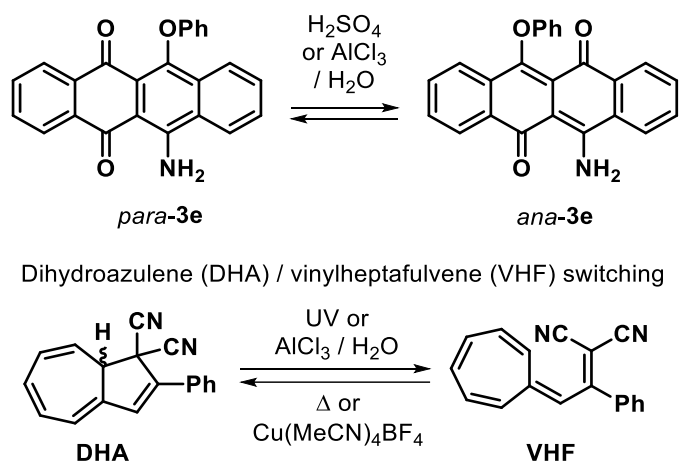
III. Switching Mechanism

The switching mechanism of PAQs was studied using different experimental techniques by the groups of Barachevsky,[86] Rentzepis,[88] Malakhov,[119] and Wirz.[63] The first experimental investigation was performed for PAQ **2** by means of laser flash photolysis ($\lambda_{ex} = 347$ nm, $\tau = 25$ ns)[86] and unsubstituted *para-* and *ana*-naphthacenequinones (**PN** and **AN**, respectively) were used as reference. It is well established that *para*-quinones such as **PN** readily cross over to their triplet state(s) via intersystem crossing (ISC) from the initially formed excited singlet state(s). However, upon excitation *para*-**2** gave a colored species with a strong hypsochromically shifted absorption (~410 nm) in comparison with **PN** (~490 nm) and thus a triplet state of the starting *para*-isomer was excluded. Interestingly, the lifetime was dependent on solvent viscosity and oxygen concentration, clearly pointing to a triplet. While in oxygen-saturated solution, the lifetime was much shorter ($\tau_{1/2} = 0.22$ μs) as compared to argon-saturated solution ($\tau_{1/2} = 4$ μs) and these

35

values were higher in triacetin. The quenching of this triplet resulted in formation of both *para*-and *ana*-**2**. The yield of *ana*-**2** was not dependent on solvent viscosity and oxygen concentration. Based on these findings, the authors proposed the biradical structure *bir*-**2** for the key triplet intermediate (Scheme 19A).
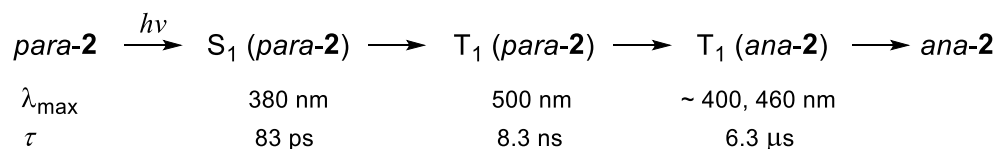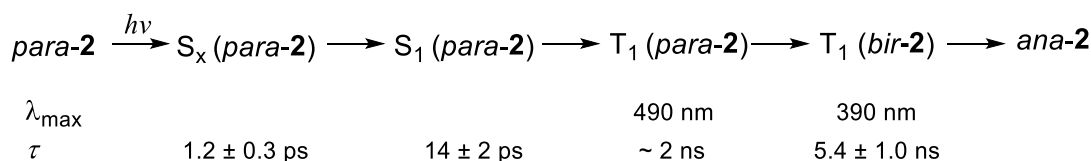
Scheme 19. Mechanism of *para*-**2** isomerization.
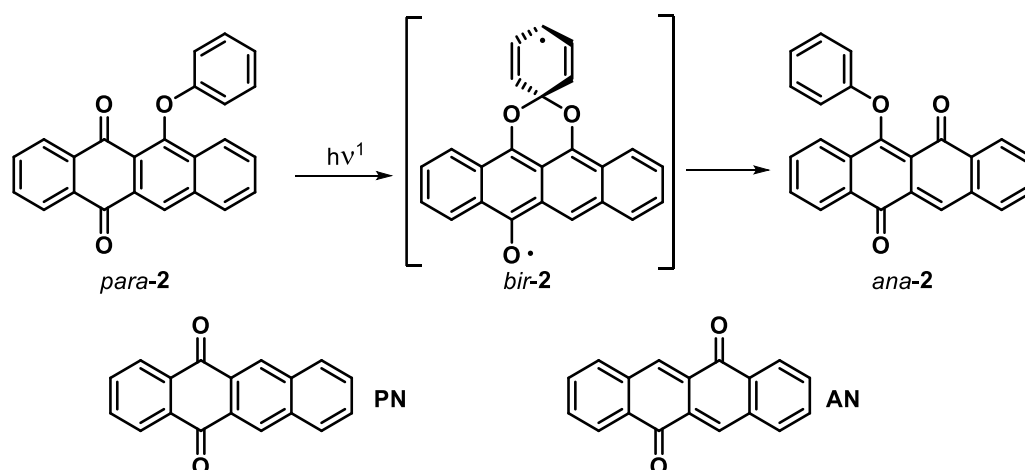
A. Mechanism, proposed by Barachevsky and coworkers:

$$para\text{-}\mathbf{2} \xrightarrow{h\nu} S_1\,(para\text{-}\mathbf{2}) \longrightarrow T_1\,(bir\text{-}\mathbf{2}) \xrightarrow{Q} ana\text{-}\mathbf{2}$$

λ_{max}		~ 410 nm
τ		0.22 µs (O$_2$)

B. Mechanism, proposed by Rentzepis and coworkers:

$$para\text{-}\mathbf{2} \xrightarrow{h\nu} S_1\,(para\text{-}\mathbf{2}) \longrightarrow T_1\,(para\text{-}\mathbf{2}) \longrightarrow T_1\,(ana\text{-}\mathbf{2}) \longrightarrow ana\text{-}\mathbf{2}$$

λ_{max}	380 nm	500 nm	~ 400, 460 nm
τ	83 ps	8.3 ns	6.3 µs

C. Mechanism, proposed by Wirz and coworkers:

$$para\text{-}\mathbf{2} \xrightarrow{h\nu} S_x\,(para\text{-}\mathbf{2}) \longrightarrow S_1\,(para\text{-}\mathbf{2}) \longrightarrow T_1\,(para\text{-}\mathbf{2}) \longrightarrow T_1\,(bir\text{-}\mathbf{2}) \longrightarrow ana\text{-}\mathbf{2}$$

λ_{max}			490 nm	390 nm
τ	1.2 ± 0.3 ps	14 ± 2 ps	~ 2 ns	5.4 ± 1.0 ns

Additional proof for the role of the triplet manifold in PAQ isomerization was obtained recently.[62] It was found that irradiation of certain PAQs in the presence of known triplet quencher, 1,4-diazabicyclo[2.2.2]octane (DABCO), did not result in the formation of corresponding *ana*-isomers.

The group of Rentzepis studied the mechanism of *para*-**2** isomerization by laser flash photolysis with enhanced time resolution (λ_{ex} = 355 nm, τ = 8 ns / 25 ps) in toluene.[88] Spiro-form

bir-**2** was excluded from their consideration and an adiabatic mechanism was proposed that involves a triplet of *ana*-**2** as the key intermediate (Scheme 19B).

Primary processes of *para*-**2** photoisomerization initiated by femtosecond laser pulses (λ_{ex} = 307 nm) were also studied.[119] The lifetime of first excited singlet state S_1 of *para*-**2**, identified as n,π^* state, was measured to be 12.5 ps in toluene. Following El Sayed's rule, intersystem crossing led to the corresponding triplet state T_1 with π,π^* character. From there the reaction pathway was mapped using semi-empirical methods calculating the energies of the relevant excited states of the *para*- and *ana*-isomers along the reaction coordinate represented by the O-C distance (Figure 15).[119] As a result of these computations, it was found that the photochemical isomerization proceeds exclusively *via* the triplet manifold with a deep minimum at the geometry corresponding to the biradical spiro-complex *bir*-**2**.
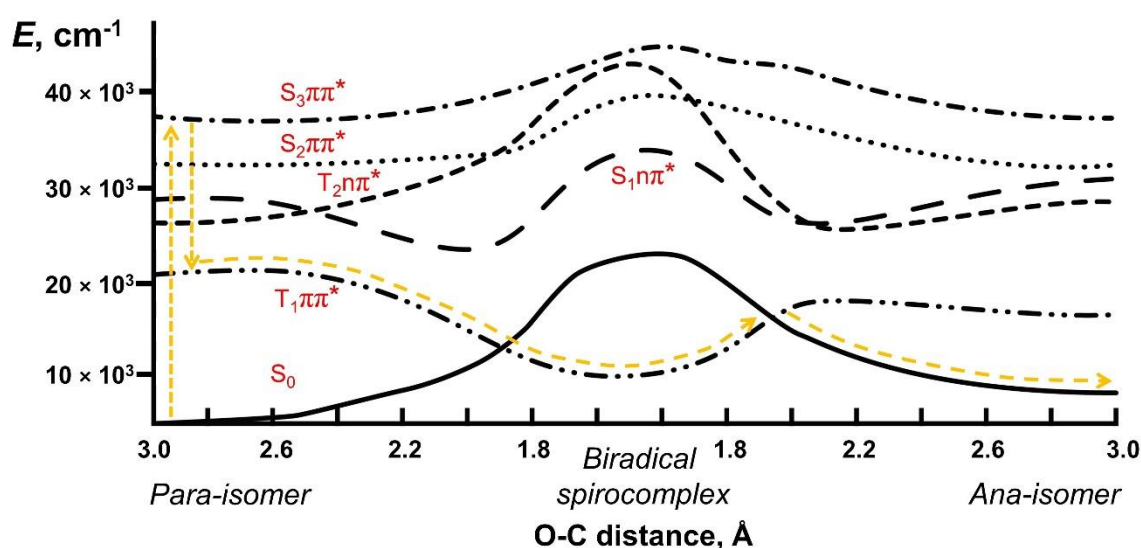

Figure 15. Potential energy surfaces for different singlet and triplet states for *para*-**2**. Adopted from [119].

The perhaps most comprehensive and insightful mechanistic investigation using various techniques was performed by Wirz and coworkers.[63] Combination of by subpicosecond pump–probe, photoacoustic, and emission spectroscopies, as well as nanosecond laser flash photolysis (λ_{ex} = 248 nm / 308 nm / 351 nm, τ = 25 ns) allowed to detect and evaluate the lifetime of a number of transient species (Scheme 19C). The key finding was the detection of a short-lived triplet state of *para*-**2** (τ ca. 2 ns) along with another triplet species (*bir*-**2**) with properties that did not matched with those of the triplet state obtained directly from *ana*-**2**. In additional experiments on triplet sensitization of *ana*-**2** by eosin Y, no *ana*-**2** → *para*-**2** conversion was detected. Thus, the reverse photoreaction proceeds directly from the lowest singlet state. Detection of triplet state of *ana*-**2** during the previous studies was rationalized as result of re-excitation of the spiro-biradical or *ana*-

37

isomer. Thus and in contrast to the conclusion of Rentzepis and coworkers,[88] the reaction proceeds *via* non-adiabatic phenyl migration. Quantum-chemical calculations of energies for three possible triplet intermediates also suggested a preference for the non-adiabatic pathway *via* triplet biradical *bir*-**2**.[120]

IV. Applications

IV.1. Photoactivated sensors

The high reactivity of *ana*-isomers towards nucleophiles can be used for the development of smart sensors activated by light on demand as introduced in recent years.[121] Early works showed a high tendency of the *ana*-isomer toward nucleophiles, amines, alcohols, and water. The reactivity towards *C*-nucleophiles was also mentioned, however, without experimental data.

The interaction of *ana*-**63** with a number of anions (CN⁻, F⁻, Cl⁻, Br⁻, I⁻, NO₃⁻, H₂PO₄⁻, and AcO⁻; *n*-Bu₄N⁺ served as a counterion in all cases) has been studied (Figure 16).[122] Significant spectral response was obtained only for cyanide ions, accompanied by emergence of an intense band in visible and near IR regions and decreasing of intensity of band corresponding to *ana*-isomer. This deeply colored intermediate (presumably, **65**) is thermally unstable, addition of acid boosts its destruction to final product **64**.
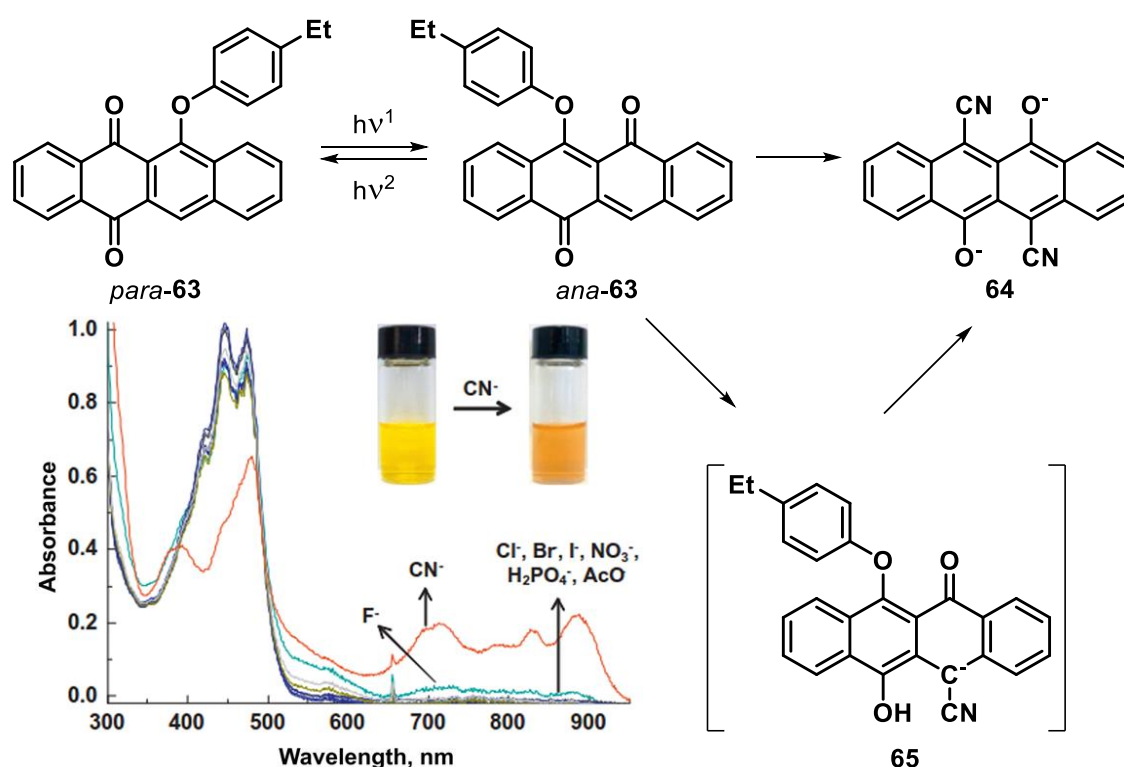

Figure 16. Photochromic transformation and changes of absorbance of photogenerated *ana*-**63** upon addition of various anions. Adapted with permission from ref. [122]. Copyright 2011 Elsevier.

38

Ana-isomers of PAQs showed selectivity towards nucleophiles, which was used to develop a sensor for amines.[100] Tertiary amines and aniline do not affect the absorbance of the irradiated solution of *para*-**12d** (compare Figures 17B and 17C). Irradiation of *para*-**12d** in the presence of primary amines results in the formation of the adducts **66** with red-shifted absorption in comparison to *ana*-**12d** (Figures 17A,C). Secondary amines cause only the hydrolysis of *ana*-isomer towards hydroxy-derivatives with blue-shifted absorption maximum.
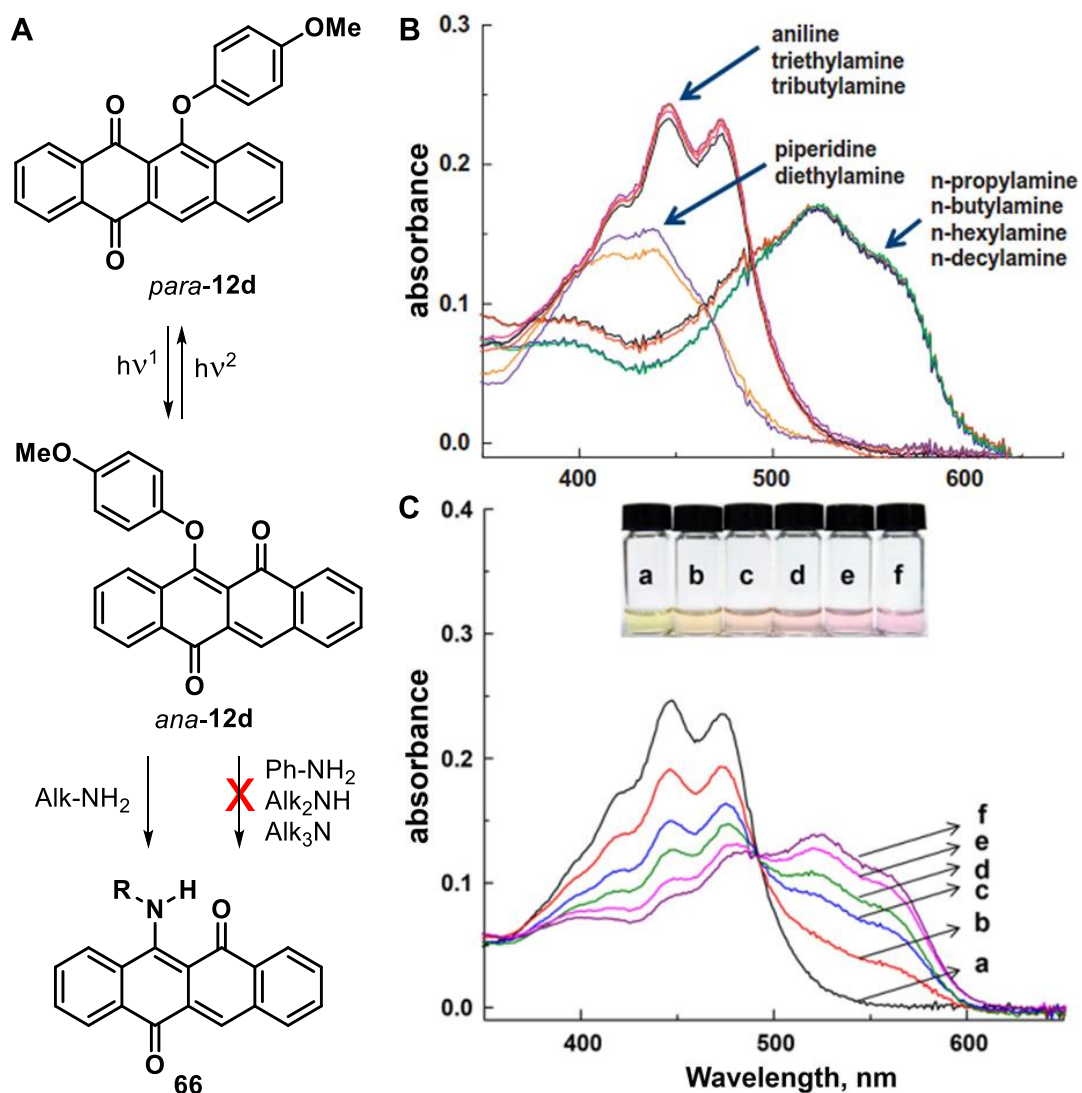

Figure 17. Chemical transformation of PAQ *para*-**12d** (A). Spectral changes of *ana*-**12d** solution in the presence of different amines (B). Spectral changes of *ana*-**14b** solution (MeCN, 25 μM) in the presence of 0 (a), 5 (b), 10(c), 15(d), 20(e), and 25 (f) μM of *n*-butylamine (C). Adapted with permission from ref. [100]. Copyright 2012 Elsevier.

39

IV.2. Cross-linking for derivatization of molecules

Highly effective and selective reactions of amines with *ana*-PAQ could be used as a tool for photocontrollable conjugation of entities with anthraquinone and amine functionalities as conceptually illustrated in Scheme 22A. In the initial state, *para*-**PAQ** cannot interact with amines yet upon photoisomerization to *ana*-**PAQ** its ability to react with amines can be activated. Using this approach, functionalities of the PAQs and amines can be covalently connected on demand.

This concept was realized for development of new crown ethers, functionalized by anthraquinone moieties (Scheme 22B). Diamino-substituted dibenzo-18-crown-6-,[123] 4-aminobenzo-15-crown-5-,[124] and 4-aminobenzo-18-crown-6[125] ethers were conjugated with PAQs by photochemically induced reaction. The obtained derivatives revealed enhanced complexation properties with alkaline and earth alkaline metals. The π-π stacking between PAQ-parts provides higher stability of 2:1 complexes of **67a** with Sr^{2+} and Ba^{2+} than the corresponding 1:1 complexes. Another interesting feature is a shift of the equilibrium of the adduct towards the oxy-imine tautomer due to the electron-withdrawing effect of the crowned metal cation on the amine nitrogen atom.

Scheme 22. Photoinduced conjugation using PAQ molecules.
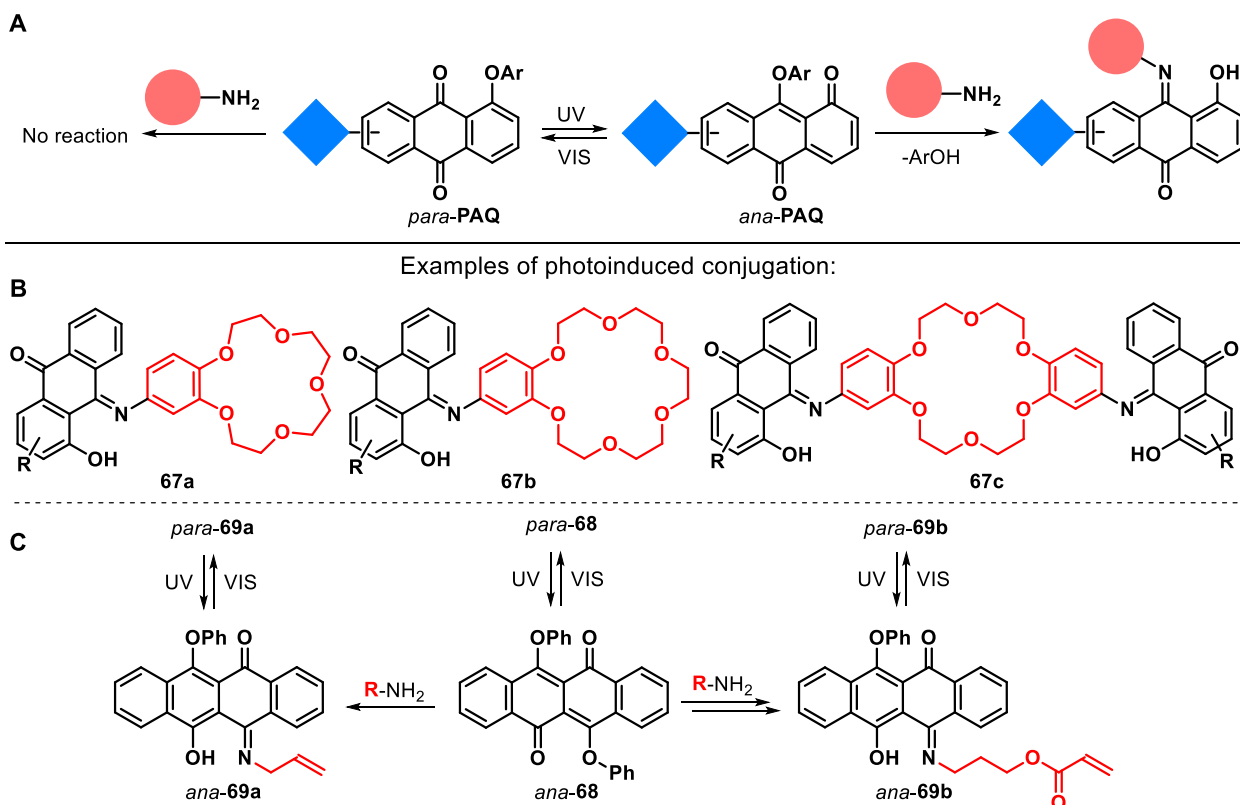
Cross-conjugation by the reaction of *ana*-isomers with amines has been applied for synthesis of PAQ-based monomers (Scheme 22C).[95] PAQ *para*-**68** has two phenoxy groups in

40

peri-positions. Treatment of the corresponding *ana*-isomer with ammonia and primary amines results in the substitution of only one phenoxy group, yet the products represent *ana*-isomers of the corresponding 6-substituted naphthacenequinones.[60] The last species are still photochromic and form *para*-isomers upon exposure to visible light. This strategy enables the synthesis of PAQ-based monomers *ana*-**69a,b**. Interestingly, the authors[95] failed to polymerize them by free-radical copolymerizaion with heptane and methyl methacrylate, correspondingly. Probably, conversion of *ana*-**69a,b** to their corresponding *para*-isomers could help to overcome this problem.

IV.3. PAQ in combination with redox active molecules

Quinone derivatives, including 1,4-benzoquinone, are of great interest for application in materials chemistry due to their unique redox properties.[126,127] Branda and coworkers reported a series of PAQ derivatives to manipulate photoinduced electron transfer (PET) from porphyrin dyes in order to develop memories with non-destructive redout. They synthesized covalent dyads **70** containing the PAQ photoswitch attached via phenylene or benzamide linkers to the *meso*-position of a tetraphenylporphyrin (Figure 18A).[128] Disappointingly, photoswitching was inhibited in these compounds most likely due to quenching of the excited state by an electron/energy transfer process from the excited PAQ to the porphyrin. In view of the ease of porphyrin oxidation – and PAQ reduction – the observed phenomenon is not unexpected and has been observed as well in a related context of an azobenzene-porphyrin dyad.[129]

To reduce the negative effect of porphyrin on photochromism PAQ, a non-covalent and thus dynamic dyad was designed.[111] Carboxyl-derived phenoxynaphthacenequinone exhibits a strong non-covalent interaction with urea-based porphyrin derivative and hence forms the corresponding dimeric complex **71** (Figure 18B). As discussed above, cyclic voltammetry shows that the *ana*-isomer is a better electron-acceptor as compared to the *para*-PAQ. PET free energy calculations moreover revealed that electron transfer from the porphyrin to the PAQ's *ana*-isomer is the more exergonic process. Thus, the fluorescence of porphyrin is quenched by the photogenerated *ana*-isomer much more efficiently, which was interpreted as more favorable electron transfer.

Efficient photoswitching of PAQ in the solid state allowed to explore the PAQ-porphyrin pair in polymeric matrices.[106] Copolymers of PAQ and porphyrin (Figure 18C) were efficiently synthesized by ROMP. In contrast to the covalently bonded dyad **70**, the polymers displayed photochromic performance, presumably due to the longer and stiffer linker separating the two entities to reduce photoinduced electron transfer. However, quenching was still possible allowing for photoregulation of fluorescence intensity (Figure 18D).
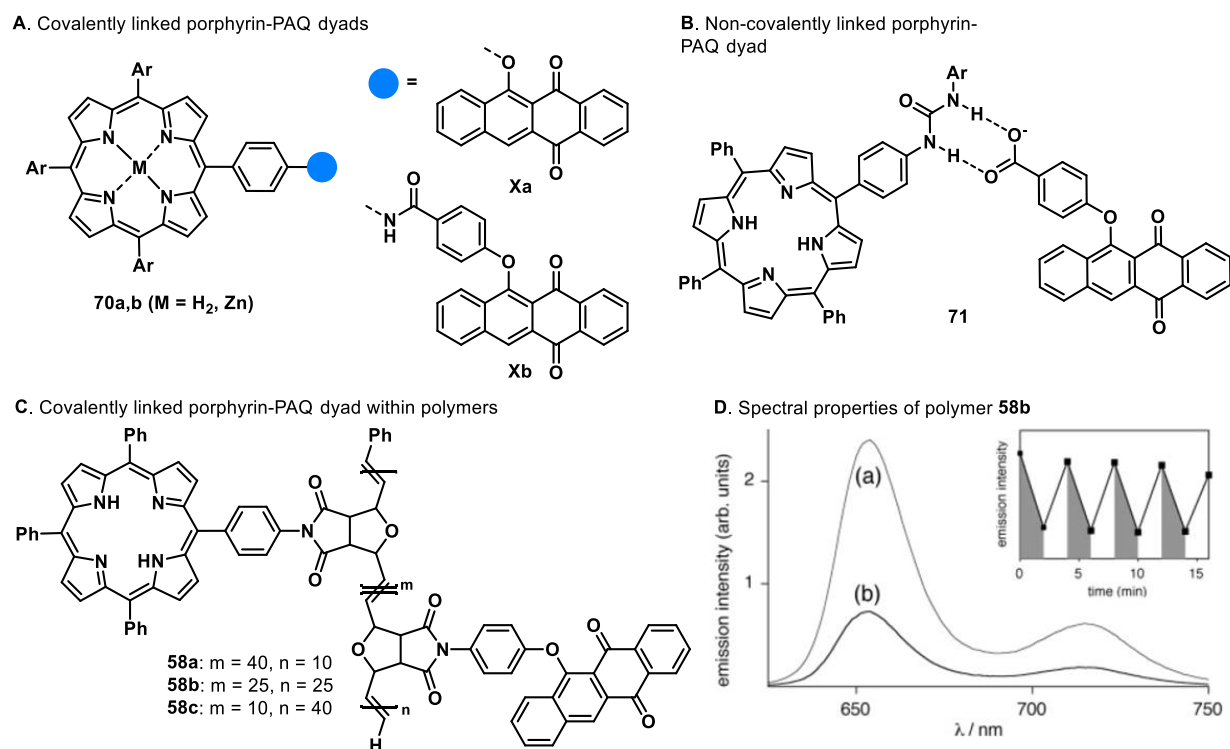
41

Figure 18. Three generations of porphyrin-PAQ hybrid molecules: covalently linked (A), non-covalently linked (B), covalently linked within polymer (C). Emission spectra of **58b** before (a) and after irradiation with UV light (D). The modulated emission signal during alternating irradiation by UV/visible light (on inset). Adapted from ref. [106] with permission of Wiley.

Differences in electron-accepting capabilities between PAQ isomers have been employed to control the intramolecular electron-transfer using UV irradiation and metal ion coordination.[112] Dyad *para*-**61** contains 6-phenoxy-5,12-naphthacenequinone as the photoswitchable unit connected with an electron-donating tetrathiafulvalene (TTF) group *via* a hexa(ethylene glycol) chain (Figure 19). According to electronic spectroscopy and cyclic voltammetry, the interaction between the TTF and PAQ fragments in **61** was negligible for both *para*- and *ana*-isomers and the dyad displayed photochromic performance typical for PAQs (Scheme 23A). Addition of metal ions (Pb^{2+}, Sc^{3+}, Zn^{2+}) to a solution of *para*-**61** led to almost no absorption spectral changes. However, in the presence of metal ions *ana*-**61** forms a complex with a long-wavelength absorbance maximum around 790 nm (Figure 19B), corresponding to the radical cation species ($TTF^{\bullet+}$) as detected by electron spin resonance spectroscopy (Figure 19C). Addition of metal ions ease the reduction of the PAQ fragment as revealed by cyclic voltammetry. Based on these findings, the authors proposed that coordination of the hexa(ethylene glycol) chains to the metal ions leads to folding and reduces the distance to facilitates intramolecular electron transfer.
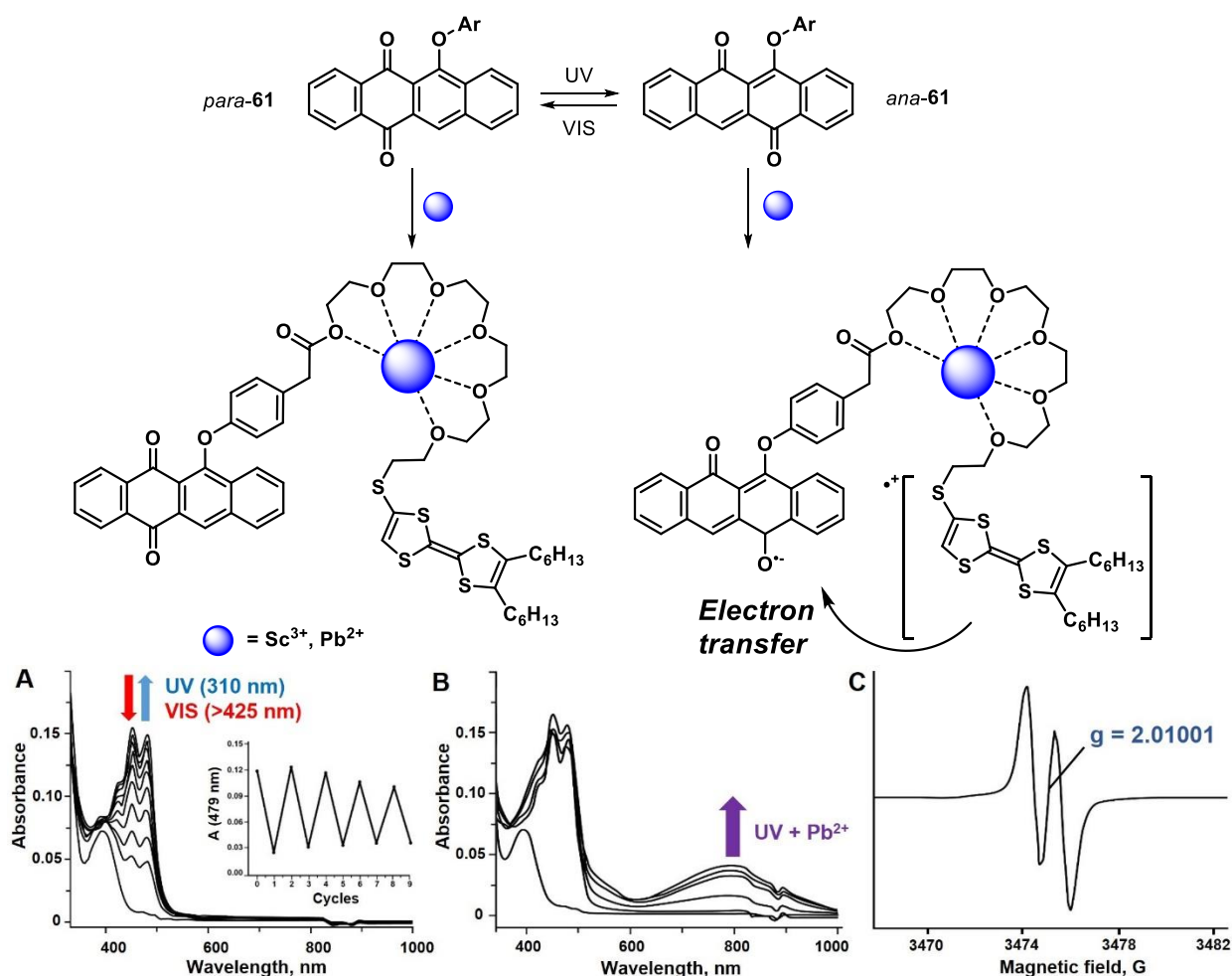
42

Figure 19. Control of intramolecular electron-transfer with UV light irradiation and metal ion coordination in PAQ-TTF dyad. Spectral changes of dyad **61** upon UV/visible light irradiation (A). Absorption spectra of **61** after UV irradiation with subsequent addition of metal salts (b). The ESR spectrum of *ana*-**61** in the presence of Pb^{2+} (c). Adapted with permission from ref. [112]. Copyright 2011 The Royal Society of Chemistry.

IV.3. Multiphotochromic systems

Molecules containing two or more photochromic fragments are refered to as multiphotochromic systems.[130,131] Interest in such systems is caused by the possibility to design molecules having more than two switching states, the interconversion between which can be triggered by light of different wavelengths, thermally or by other stimuli. PAQs have been tested in the context of developing advanced multiphotochromic systems.

The first hybrid employed PAQ was **72a**, containing azobenzene as migrating group (Figure 20A).[65] Upon UV irradiation of **72a**, significant changes in absorption were observed. Comparison of spectral changes with other PAQs (Figures 4 and 8) suggests that a prominent band at 352 nm in the spectrum of **72a** is related to the azobenzene moiety, and its conversion to a blue-shifted band is reminiscent of the *E*/*Z*-isomerization process within the parent azobenzene unit.[132]

43

However, using the irreversible reaction of the photoinduced species with ammonia (see Figure 5) disclosed formation of the corresponding *ana*-isomer reaching 16% conversion in the PSS. Thus, in this system, both processes, arylotropy and *E/Z*-isomerization have been observed. Similar results were obtained for analogues **72b-d** with various substituents in the *para*-position.[133]
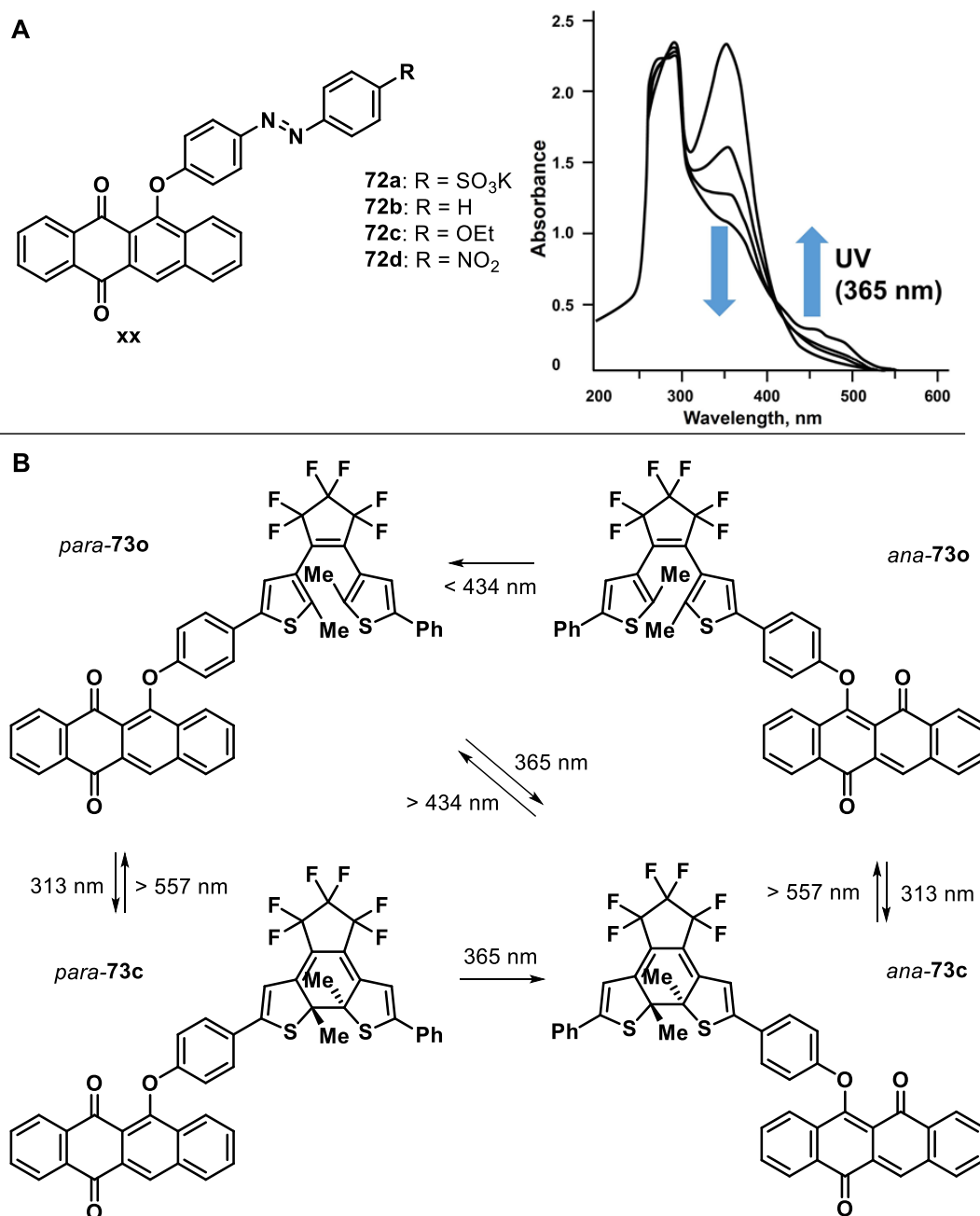

Figure 20. Multiphotochromic systems based on PAQs. Hybrids with azobenzene and spectral changes upon irradiation of **72a** in DMSO by UV light (365 nm) (A). Adapted from ref. [65] with permission of Elsevier. Multicolor switching of PAQ/diarylethene dyad (B).

44

Branda and coworkers studied combination of PAQ and diarylethenes (Figure 20B).[134] As mentioned above, both photoswitch families possess similar properties, including positive photochromism and thermally stable photoisomers. Importantly, the absorption bands of these two chromophores are separated enough to be able to induce selective diarylethene cyclization (*para*-**73o** → *para*-**73c**) and cycloreversion (*para*-**73c** → *para*-**73o**) by 313 nm and >557 nm light, respectively. Notably, manipulation of such molecular systems with different wavelengths made it possible to realize four-state switches selectively addressable by light only.

IV.4. Interface materials

Willner and coworkers have developed PAQ-derived gold electrodes as new type of stimuli responsive and sensitive interface materials.[135] Naphthacenequinone-based photoswitch **74** was covalently connected to the gold electrodes *via* cystamine linkers (Figure 21A).[61] To avoid ill-defined redox properties as a result of non-dense packing, a rigid monolayer assembly was constructed by additional treatment of the surface with 1-tetradecanethiol. Surprisingly, only the electrode in the *para*-state was electrochemically active with well-defined, quasi-reversible redox wave at -0.62 V vs. saturated calomel electrode (SCE). Effective photoisomerization of the monolayer was achieved by UV irradiation (340 nm < λ < 360 nm). The PSS of the irradiated monolayer was proven to be nearly quantitative. The cyclic voltammogram reveals only the background current of the electrolyte (Figure 21B). Thus, the *ana*-state of the electrode is electrochemically inactive. Visible light irradiation resulted in restoration of initial redox properties and at least 10 switching cycles could be performed without any detectable fatigue. Since electron transfer is often coupled to proton transfer, it does not come a surprise that redox properties of the monolayer electrode were found to be pH-sensitive. Upon increasing the pH, a negative shift of the redox curve was observed and explained by the proton-coupled reduction of *para*-**74** within the monolayer involving two electrons and two protons.

The redox properties of the interface were applied to develop a light-triggered electrocatalytic system (Figure 21C).[136] The primary redox process of the *para*-**74** was coupled with an enzyme-catalyzed reaction, i.e., electrochemical reduction of nitrate anions catalyzed by nitrate reductase (NR). At the first step, electrochemically reduced *para*-**74** mediated electrochemical reduction of *N*,*N*′-dibenzyl-4,4′-bipyridinium (BV). In turn, the latter participated in enzyme reduction and activation of nitrate → nitrite reduction. Photoisomerization of the PAQ resulted in complete prevention of BV reduction and deactivation of the catalytic cycle.
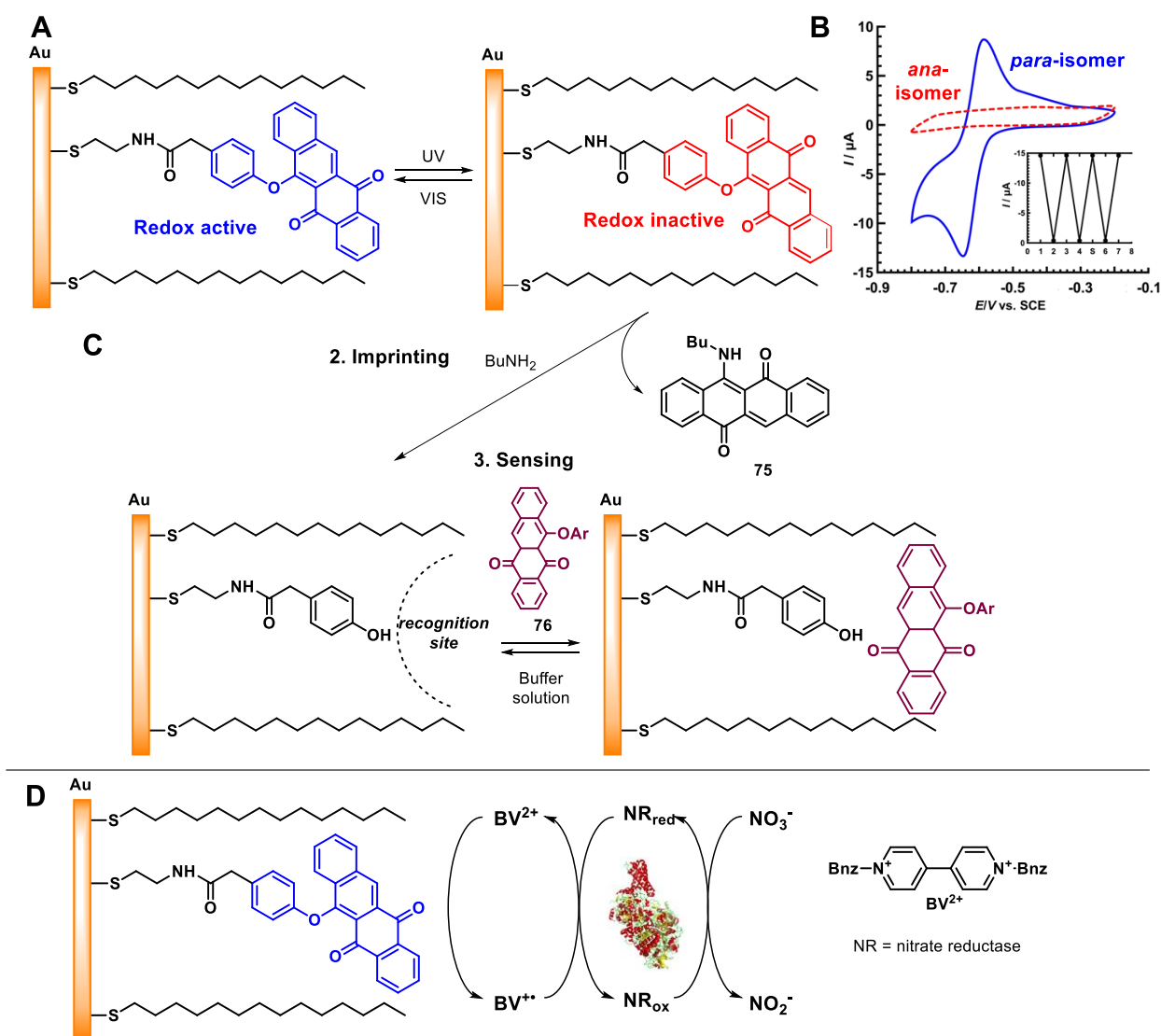
Figure 21. Electroactive PAQ-based photoisomerizable monolayer-electrode. Photoswitching (A) and cyclic voltammetry of the different states and multiple photoswitching (on inset) (B). Adapted from ref. [135b] with permission of Wiley. Photochemical imprinting of molecular recognition sites in monolayers and the recognition of the guest PAQ molecule (C). Participation of PAQs-photoisomerizable monolayer electrodes in cascade biocatalytic process (D). Use in accordance with CC BY 3.0 license.

The PAQ-based monolayers assembled on gold electrodes were used for development of materials with imprinted molecular recognition sites (Scheme 25D).[137,138] Treatment of the pre-irradiated electrodes with a nucleophilic reagent (*n*-butylamine) resulted in the elimination of quinone-based molecules from the monolayer in the form of 6-(butylamino)tetracene-5,11-dione (Figure 21C). At the same time, the phenol part of the initial PAQ-molecule persisted on the gold surface. Detachment of the quinone molecule can be considered as an *imprinting* process. It leaves

46

a recognition site on the surface, representing a relatively large cavity with additional phenolic hydroxyl group at the "bottom". It was found that molecule **76** ideally fits in the recognition site forming a relatively stable complex, which was proven by cyclic voltammetry and microgravimetric quartz-crystal-microbalance analysis. Association was found to be reversible since in neat buffer solution, the guest molecules dissociate again. Recognition was shown to be selective as addition of a number of anthraquinone, naphthoquinone, bipyridinium instead of **76** did not result in detectable host-guest interactions.

V. Conclusion and Outlook

"Knowledge is not simply another commodity. On the contrary. Knowledge is never used up. It increases by diffusion and grows by dispersion."

This quote by Daniel J. Boorstin points out a general problem when a field of research becomes mature and established. After the initial discovery of the phenomenon in the mid 19th century and development of the main classes of photochromic compounds, i.e. azobenzenes, spiropyrans, and diarylethenes, the field of molecular photochromism has been blossoming in recent years. However, most researchers have been using and further optimizing compounds of these few established compound families, thereby ignoring the fact that there are other, less prominent classes of photoswitches that indeed may offer unique advantages. Among them are for example indigos[139] and indigoids[26b] but also the PAQs reviewed herein can serve as interesting alternatives. From the previous sections it becomes clear that there are some key features of this interesting and often neglected family of photochromic compounds including:

- Thermal bistability: The available qualitative data indicate that PAQ photoswitches convert to thermally stable *ana*-isomers, which provide a means of non-volatile storage.
- Chemical sensitivity: The thermally stable *ana*-isomers are sensitive to the presence of nucleophiles, thereby allowing the development of photoactivated sensors and drugs.
- Solid state switching: Photoswitchability of PAQs is retained in the solid state, including crystals and polymers, rendering these compounds applicable in materials and devices.
- Light-induced electronic modulation: The considerable modulation of their frontier molecular orbital levels make PAQs attractive for application in molecular electronics,[140] e.g. fabrication of light-programmable transistor devices, including OFET (organic field-effect transistors) and OLET (organic light-emitted transistors).[141]

47

Of course, various aspects of this photoswitch family remain to be investigated. For example, it should be noted that the photogenerated, sensitive *ana*-isomers of PAQ photoswitches have only scarcely been studied by ^{1}H NMR spectroscopy.[142] Moreover, these species have thus far not been characterized by X-ray crystallography. From these limited data, it becomes clear that more insightful structural data, in particular of the *ana*-isomer, need to be gathered.

Besides obtaining a deeper and thorough understanding of this interesting photoswitch family, it should be explored in various suitable applications, i.e. settings in which the use of PAQ photoswitches provides a unique advantage. This could for example be visible light activated release of small molecules for various purposes.[143] But also the exploration of PAQs within electronic (hybrid) materials promises to be a fruitful line of research for potential future applications. In addition, the photogenerated reactivity of PAQs could be used for implementation of dynamic covalent bonds[144] by using phenols as nucleophilic species.

Through this review, we intend to make the community and in particular its most recent protagonists aware of this rather forgotten class of photochromic compounds. We hope that it will serve as a valuable source of inspiration for researchers and help to broaden the knowledge base in the field of molecular photochromism.

VI. References

[1] H. Bouas-Laurent, H. Dürr, *Pure Appl. Chem.* **2001**, *73*, 639–665 (DOI: 10.1351/pac200173040639).

[2] (a) A. Goulet-Hanssens, F. Eisenreich, S. Hecht, *Adv. Mater.* **2020**, *32*, 1905966 (DOI: 10.1002/adma.201905966). (b) Photochromic Materials: Preparation, Properties and Applications. H. Tian, J. Zhang, Eds. 2016, Wiley. (c) Z. L. Pianowski, *Chem. Eur. J.* **2019**, *25*, 5128-5144 (DOI: 10.1002/chem.201805814).

[3] (a) Y. Hirshberg, *J. Am. Chem. Soc.* **1956**, 78, 10, 2304–2312 (DOI: 10.1021/ja01591a075). (b) V. A. Barachevsky, Yu. P. Strokach, Yu. A. Puankov, M. M. Krayushkin, *J. Phys. Org. Chem.* **2007**, 20, 1007-1020 (DOI: 10.1002/poc.1191).

[4] (a) W. A. Velema, W. Szymanski, B. L. Feringa, *J. Am. Chem. Soc.* **2014**, *136*, 2178–2191 (DOI: 10.1021/ja413063e). (b) J. Broichhagen, J. A. Frank, D. Trauner, *Acc. Chem. Res.* **2015**, *48*, 1947–1960 (DOI: 10.1021/acs.accounts.5b00129). (c) K. Hull, J. Morstein, D. Trauner, *Chem. Rev.* **2018**, *118*, 10710–10747 (DOI: 10.1021/acs.chemrev.8b00037). (d) M. M. Lerch, M. J. Hansen, G. M. van Dam, W. Szymanski, B. L. Feringa, *Angew. Chem. Int. Ed.* **2016**, *55*, 10978-10999 (DOI: 10.1002/anie.201601931).

[5] J. Volarić, W. Szymanski, N. A. Simeth, B. L. Feringa, *Chem. Soc. Rev.* **2021**, *50*, 12377-12449 (DOI: 10.1039/D0CS00547A).

[6] (a) B. M. Neilson, C. W. Bielawski, *ACS Catal.* **2013**, *3*, 1874–1885 (10.1021/cs4003673); (b) D. Majee, S. Presolski, *ACS Catal.* **2021**, *11*, 2244–2252 (10.1021/acscatal.0c05232); (c) I. Jablonkai, A. Kunfi, D.-H. Qu, G. London, *Chapter Seven - A new color in green chemistry: Photochromic molecular switches as components of multifunctional catalytic systems* in Nontraditional Activation Methods in Green and Sustainable Applications, Advances in Green and Sustainable Chemistry **2021**, Pages 241-282 (10.1016/B978-0-12-819009-8.00006-2).

[7] M. Regehly, Y. Garmshausen, M. Reuter, N. F. König, E. Israel, D. P. Kelly, C.-Y. Chou, K. Koch, B. Asfari, S. Hecht, *Nature* **2020**, *588*, 620-624 (DOI: 10.1038/s41586-020-3029-7).

[8] G. A. Leith, C. R. Martin, A. Mathur, P. Kittikhunnatham, K. Chul Park, N. B. Shustova, *Adv. Energy Mater.* **2021**, 2100441 (DOI: 10.1002/aenm.202100441).

[9] X. Huang, T. Li, *J. Mater. Chem. C* **2020**, *8*, 821-848 (DOI: 10.1039/C9TC06054E).

[10] A. M. Rice, C. R. Martin, V. A. Galitskiy, A. A. Berseneva, G. A. Leith, N. B. Shustova, *Chem. Rev.* **2020**, *120*, 8790-8813 (DOI: 10.1021/acs.chemrev.9b00350).

[11] D. Kitagawa, C. J. Bardeen, S. Kobatake, *Symmetry* **2020**, *12*, 1478 (DOI: 10.3390/sym12091478).

[12] D. Liu, D. J. Broer, *Liq. Cryst. Rev.* **2013**, *1*, 20–28 (DOI: 10.1080/21680396.2013.766410).

[13] S. Chen, R. Costil, F. King-Chi Leung, B. L. Feringa, *Angew. Chem. Int. Ed.* **2021**, *60*, 11604-11627 (DOI: 10.1002/anie.202007693).

[14] M. Irie, T. Fukaminato, K. Matsuda, S. Kobatake, *Chem. Rev.* **2014**, *114*, 12174-12277 (DOI: 10.1021/cr500249p).

[15] (a) Y. Yokoyama, *Chem. Rev.* **2000**, *100*, 1717–1740 (DOI: 10.1021/cr980070c). (b) D. Lachmann, R. Lahmy, B. König, *Eur. J. Org. Chem.* **2019**, 5018-5024 (DOI: 10.1002/ejoc.201900219).

[16] (a) H. M. D. Bandara, S. C. Burdette, *Chem. Soc. Rev.* **2012**, *41*, 1809-1825 (DOI: 10.1039/C1CS15179G). (b) S. Crespi, N. A. Simeth, B. König, *Nat. Rev. Chem.* **2019**, *3*, 133–146 (DOI: 10.1038/s41570-019-0074-6).

[17] (a) V. I. Minkin, *Chem. Rev.* **2004**, *104*, 2751–2776 (DOI: 10.1021/cr020088u). (b) L. Kortekaas, W. R. Browne, *Chem. Soc. Rev.* **2019**, *48*, 3406-3424 (DOI: 10.1039/C9CS00203K). (c) R. Klajn, *Chem. Soc. Rev.* **2014**, *43*, 148-184 (DOI: 10.1039/C3CS60181A).

[18] J. D. Harris, M. J. Moran, I. Aprahamian, *Proc. Natl. Acad. Sci. USA* **2018**, *115*, 9414-9422 (DOI: 10.1073/pnas.1714499115).

[19] (a) M. M. Lerch, W. Szymański, B. L. Feringa, *Chem. Soc. Rev.* **2018**, *47*, 1910-1937 (DOI: 10.1039/C7CS00772H). (b) R. Berraud-Pache, E. Santamaría-Aranda, B. De Souza, G. Bistoni, F. Neese, D. Sampedro, R. Izsak, *Chem. Sci.* **2021**, *12*, 2916-2924 (DOI: 10.1039/D0SC06575G).

[20] (a) R. Siewertsen, H. Neumann, B. Buchheim-Stehn, R. Herges, C. Näther, F. Renth, F. Temps, *J. Am. Chem. Soc.* **2009**, *131*, 15594–15595 (DOI: 10.1021/ja906547d). (b) M. Hammerich, C. Schütt, C. Stähler, P. Lentes, F. Röhricht, R. Höppner, R. Herges, *J. Am. Chem. Soc.* **2016**, *138*, 13111–13114 (DOI: 10.1021/jacs.6b05846).

[21] (a) B. Shao, I. Aprahamian, *Chem* **2020**, *6*, 2162-2173 (DOI: 10.1016/j.chempr.2020.08.007). (b) I. Aprahamian. *Chem. Commun.* **2017**, *53*, 6674-6684 (DOI: 10.1039/C7CC02879B). (c) D. J. van Dijken, P. Kovaříček, S. P. Ihrig, S. Hecht. *J. Am. Chem. Soc.* **2015**, *137*, 14982-14991 (DOI: 10.1021/jacs.5b09519).

[22] (a) M. W. H. Hoorens, M. Medved', A. D. Laurent, M. Di Donato, S. Fanetti, L. Slappendel, M. Hilbers, B. L. Feringa, W. Jan Buma, W. Szymanski, *Nat. Commun.* **2019**, *10*, 2390 (DOI: 10.1038/s41467-019-10251-8). (b) S. Crespi, N. A. Simeth, M. Di Donato, S. Doria, C. N. Stindt, M. F. Hilbers, F. L. Kiss, R. Toyoda, S. Wesseling, W. Jan Buma, B. L. Feringa, W. Szymański, *Angew. Chem. Int. Ed.* **2021**, (DOI: 10.1002/ange.202111748).

[23] S. Kirchner, A.-L. Leistner, P. Gödtel, A. Seliwjorstow, S. Weber, J. Karcher, M. Nieger, Z. Pianowski, *Nat. Commun.* **2022**, *13*, 6066 (DOI: 10.1038/s41467-022-33750-7).

[24] T. T. Ngoc, N. Grabicki, E. Irrana, O. Dumele, J. F. Teichert, *Nature Chem.* **2023**, *15*, 377–385 (DOI: 10.1038/s41557-022-01121-w).

[25] (a) C.-Y. Huang, A. Bonasera, L. Hristov, Y. Garmshausen, B. M. Schmidt, D. Jacquemin, S. Hecht, *J. Am. Chem. Soc.* **2017**, *139*, 15205-15211 (DOI: 10.1021/jacs.7b08726). (b) S. Thumser, L. Köttner, N. Hoffmann, P. Mayer, H. Dube, *J. Am. Chem. Soc.* **2021**, *143*, 18251–18260 (DOI: 10.1021/jacs.1c08206).

[26] (a) Wiedbrauk, S.; Dube, H. *Tetrahedron Lett.* **2015**, *56*, 4266−4274 (DOI: 10.1016/j.tetlet.2015.05.022). (b) C. Petermayer, H. Dube, *Acc. Chem. Res.* **2018**, *51*, 1153–1163 (DOI: 10.1021/acs.accounts.7b00638).

[27] K. Klaue, W. Han, P. Liesfeld, F. Berger, Y. Garmshausen, S. Hecht, *J. Am. Chem. Soc.* **2020**, *142*, 11857-11864 (DOI: 10.1021/jacs.0c04219).

[28] S. Dong, A. Ong, C. Chi, *J. Photochem. Photobiol. C* **2019**, *38*, 27-46 (DOI: 10.1016/j.jphotochemrev.2018.12.002).

[29] D. Villarón, S. J. Wezenberg, *Angew. Chem. Int. Ed.* **2020**, *59*, 13192-13202 (DOI: 10.1002/anie.202001031).

[30] S. Lin, K. G. Gutierrez-Cuevas, X. Zhang, J. Guo, Q. Li, *Adv. Funct. Mater.* **2020**, 2007957 (DOI: 10.1002/adfm.202007957).

[31] Y. Kobayashi, J. Abe, *Chem. Soc. Rev.* **2022**, *51*, 2397-2415 (DOI: 10.1039/D1CS01144H).

[32] A. Gonzalez, E.S. Kengmana, M.V. Fonseca, G.G.D. Han, *Mater. Today Adv.* **2020**, *6*, 100058 (DOI: 10.1016/j.mtadv.2020.100058).

[33] V. Shibaev, A. Bobrovsky, N. Boiko, *Prog. Polym. Sci.* **2003**, *28*, 729-836 (DOI: 10.1016/S0079-6700(02)00086-2).

[34] B. Rösner, M. Milek, A. Witt, B. Gobaut, P. Torelli, R. H. Fink, M. M. Khusniyarov, *Angew. Chem. Int. Ed.* **2015**, *54*, 12976–12980 (DOI: 10.1002/anie.201504192).

[35] R. Hayakawa, K. Higashiguchi, K. Matsuda, T. Chikyow, Y. Wakayama, *ACS Appl. Mater. Interfaces* **2013**, *5*, 3625−3630 (DOI: 10.1021/am400030z).

[36] M. Morimoto, M. Irie. *J. Am. Chem. Soc.* **2010**, *132*, 14172–14178 (DOI: 10.1021/ja105356w).

[37] E. A. Dolgopolova, V. A. Galitskiy, C. R. Martin, H. N. Gregory, B. J. Yarbrough, A. M. Rice, A. A. Berseneva, O. A. Ejegbavwo, K. S. Stephenson, P. Kittikhunnatham, S. G. Karakalos, M. D. Smith, A. B. Greytak, S. Garashchuk, N. B. Shustova, *J. Am. Chem. Soc.* **2019**, *141*, 5350−5358 (DOI: 10.1021/jacs.8b13853).

[38] M. Kathan, P. Kovařiček, C. Jurissek, A. Senf, A. Dallmann, A. F. Thünemann, S. Hecht, *Angew. Chem. Int. Ed.* **2016**, *55*, 13882–13886 (DOI: 10.1002/anie.201605311).

[39] A. Bobrovsky, V. Shibaev, A. Bubnov, V. Hamplová, M. Kašpar, M. Glogarová, *Macromolecules* **2013**, *46*, 4276–4284 (DOI: 10.1021/ma401010t).

[40] Yu. E. Gerasimenko, N. T. Poteleshchenko, *Zh. Vses. Khim. Ova.* **1971**, *16*, 105 (in Russian).

51

[41] V. N. Kostylev, B. E. Zaitsev, V. A. Barachevskii, N. T. Poteleshchenko, Yu. E. Gerasimenko, *Opt. Spektrosk.* **1971**, *30*, 86-89 (in Russian).

[42] Yu. E. Gerasimenko, in: Organic Photoswitches (A. V. El'tsov, ed.), pp. 224-233, Khimiya, Leningrad (1982) (Russ.); Organic Photoswitches (A. V. El'tsov, ed.), pp. 210-219, Consultants Bureau, New York (1990).

[43] N. T. Sokolyuk, V. V. Romanov, L. P. Pisulina, *Russ. Chem. Rev.* **1993**, *62*, 1005-1024 (DOI: 10.1070/RC1993v062n11ABEH000061).

[44] N. P. Gritsan, *Mol. Cryst. Liq. Cryst.* **1994**, *246*, 103-106 (DOI: 10.1080/10587259408037795).

[45] V. A. Barachevsky, *Mol. Cryst. Liq. Cryst.* **1994**, *246*, 95-102 (DOI: 10.1080/10587259408037794).

[46] V. A. Barachevsky, Photochromic Quinones, in Organic Photochromic and Thermochromic Compounds, Vol. 1. J. C. Crano, R. Guglielmetti, Eds. Plenum Press, New York, 1999.

[47] (a) D. Bléger, S. Hecht, *Angew. Chem., Int. Ed.* **2015**, *54*, 11338–11349 (DOI: 10.1002/anie.201500628). (b) S. Jia, W.-K. Fong, B. Graham, B. J. Boyd, *Chem. Mater.* **2018**, *30*, 2873–2887 (DOI: 10.1021/acs.chemmater.8b00357). (c) Z. Zhang, W. Wang, M. O'Hagan, J. Dai, J. Zhang, H, Tian, *Angew. Chem. Int. Ed.* **2022**, *61*, e202205758 (DOI: 10.1002/anie.202205758).

[48] M. Kathan, S. Hecht, *Chem. Soc. Rev.* **2017**, *46*, 5536-5550 (DOI: 10.1039/c7cs00112f).

[49] N. P. Tsvetkov, E. Gonzalez-Rodriguez, A. Hughes, G. dos Passos Gomes, F. D. White, F. Kuriakose, I. V. Alabugin, *Angew. Chem. Int. Ed.* **2018**, *57*, 3651-3655 (DOI: 10.1002/anie.201712783).

[50] Gerasimenko, Y. E.; Poteleschenko, N. T. *Zh. Org. Khim.* **1973**, *9*, 2392-2395 (in Russian).

[51] Y. E. Gerasimenko, A. A. Parshutkin, N. T. Poteleshchenko, V. V. Romanov, *J. Appl. Spectrosc.* **1979**, *30*, 691–693 (Russ: *Zh. Prikl. Spektrosk.* **1979**, *30*, 954-956) (DOI: 10.1007/BF00608442).

[52] Y. Yokoyama, S. Fukui, Y. Yokoyama, *Chem. Lett.* **1996**, 355-356 (DOI: 10.1246/cl.1996.355).

[53] Yu. E. Gerasimenko, N. T. Poteleshchenko, *Zh. Org. Khim.* **1971**, *7*, 2413-2415 (in Russian).

[54] Koroteev, N. I.; Magnitskii, S. A.; Shubin, V. V.; Sokolyuk, N. T. *Jpn. J. Appl. Phys.* **1997**, *36*, 424-425 (DOI: 10.1143/JJAP.36.424).

[55] E. A. Kolodina, M. S. Shvartsberg, N. P. Gritsan, *Mendeleev Commun.* **2008**, *18*, 302–304 (DOI: 10.1016/j.mencom.2008.11.004).

[56] A. E. Shchekotikhin, E. K. Shevtsova, Yu. N. Luzikov, V. A. Barachevskii, V. F. Traven', *Russ. J. Org. Chem.* **2008**, *44*, 855–862 (DOI: 10.1134/S1070428008060134).

[57] Yu. E. Gerasimenko, N. T. Poteleshchenko, *Zh. Org. Khim.* **1979**, *15*, 393-396 (in Russian).

[58] L. Köttner, E. Ciekalski, H. Dube, *Angew. Chem. Int. Ed.* **2023**, e202312955 (DOI: 10.1002/anie.202312955).

[59] Yu. E. Gerasimenko, N. T. Poteleshenko, *Zh. Org. Khim.* **1982**, *18*, 1039-1043 (in Russian).

[60] Yu. E. Gerasimenko, N. T. Poteleshchenko, V. V. Romanov, *Zh. Org. Khim.* **1980**, *16*, 1938-1945 (in Russian).

[61] A. Doron, E. Katz, M. Portnoy, I. Willner, *Angew. Chem. Int. Ed.* **1996**, *35*, 1535-1537 (DOI: 10.1002/anie.199615351).

[62] V. N. Bykov, S. A. Ukhanev, I. A. Ushakov, A. V. Vologzhanina, E. A. Antsiferov, L. S. Klimenko, A. G. Lvov, *manuscript in preparation*.

[63] R. Born, W. Fischer, D. Heger, B. Tokarczyk, J. Wirz, *Photochem. Photobiol. Sci.* **2007**, *6*, 552–559 (DOI: 10.1039/b618661k).

[64] A. Zelichenok, F. Buchholz, E. Fischer, J. Ratner, V. Krongauz, H. Anneser, C. Bräuchle, *J. Photochem. Photobiol. A* **1993**, *76*, 135-141 (DOI: 10.1016/1010-6030(93)80185-C).

[65] Z. Fang, S.-z. Wang, Z.-f. Yang, B. Chen, F.-t. Li, J.-q. Wang, S.-x. Xu, Z.-j. Jiang, T.-r. Fang, *J. Photochem. Photobiol. A* **1995**, 88, 23-30 (DOI: 10.1016/1010-6030(94)03990-C).

[66] Yu. E. Gerasimenko, N. T. Sokolyuk, L. P. Pisulina, *Zh. Org. Khim.* **1983**, *19*, 1312-1316 (in Russian).

[67] Yu. E. Gerasimenko, N. T. Sokolyuk, L. P. Pisulina, *Zh. Org. Khim.* **1985**, *21*, 453-454 (in Russian).

[68] N. T. Sokolyukl, L. P. Pisulina, *Russ. J. Org. Chem.* **2002**, *38*, 1212-1213 (DOI: 10.1023/A:1020978215981).

[69] N. T. Sokolyuk, L.P. Pisulina, *Zh. Org. Khim.* **1992**, *28*, 2193-2200 (in Russian).

[70] N. T. Sokolyuk, L.P. Pisulina, *Zh. Org. Khim.* **1994**, *30*, 447-452 (in Russian).

[71] Yu. E. Gerasimenko, N. T. Sokolyuk, L. P. Pisulina, *Zh. Org. Khim.* **1986**, *22*, 632-636 (in Russian).

[72] L. S. Klimenko, E. A. Pritchina, N. P. Gritsan, *Chem. Eur. J.* **2003**, *9*, 1639-1644 (DOI: 10.1002/chem.200390188).

[73] M. S. Shvartsberg, E. A. Kolodina, unpublished data.

[74] Yu. E. Gerasimenko, N. T. Poteleshchenko, V. V. Romanov, *Zh. Org. Khim.* **1978**, *14*, 2387-2391 (in Russian).

[75] E. P. Fokin, S. A. Russkikh, L. S. Klimenko, *Zh. Org. Khim.* **1977**, *13*, 2010-2011 (in Russian).

[76] E. P. Fokin, S. A. Russkikh, L. S. Klimenko, V. V. Russkikh, *Izv. Sib. Otd. Akad. Nauk SSSR, Khim.* **1978**, 110-120 (in Russian).

[77] E. P. Fokin, S. A. Russkikh, L. S. Klimenko, *Izv. Sib. Otd. Akad. Nauk SSSR, Ser. Khim.* **1979**, *9*, 11-124 (in Russian)

[78] E. P. Fokin, L. S. Klimenko, S. A. Russkikh, N. P. Gritsan, Izv. *Sib. Otd. Akad. Nauk SSSR, Ser. Khim. Nauk* **1981**, *12*, 116-125 (in Russian).

[79] V. A. Barachevsky, N. T. Sokolyuk, et al. Unpublished data.

80 V.I. Eroshkin, E. P. Fokin, A. I. Volkov, T. A. Andreeva, L. S. Klimenko, Yu. K. Dolgikh, A. F. Simonenko, *Zh. Fiz. Khim.* **1991**, *65*, 1479-1484 (in Russian).

81 V. A. Litvinov, L. S. Klimenko, *Vest. Yugor. Gos. Univer.* **2016**, *12*, 12-19 (in Russian) (DOI: 10.17816/byusu201612312-19).

82 (a) R. Asato, C. J. Martin, T. Nakashima, J. P. Calupitan, G. Rapenne, T. Kawai, *J. Phys. Chem. Lett.* **2021**, *12*, 11391–11398 (10.1021/acs.jpclett.1c03052). (b) J. Gurke, M. Quick, N. P. Ernsting, S. Hecht, *Chem. Commun.* **2017**, *53*, 2150-2153 (DOI: 10.1039/c6cc10182h). (c) Z. Wang, J. Udmark, K. Börjesson, R. Rodrigues, A. Roffey, M. Abrahamsson, M. B. Nielsen, K. Moth-Poulsen, *ChemSysChem* **2017**, *10*, 3049-3055 (DOI: 10.1002/cssc.201700679).

83 Z. Wang, P. Erhart, T. Li, Z.-Y. Zhang, D. Sampedro, Z. Hu, Hermann A. Wegner, Olaf Brummel, J. Libuda, M. B. Nielsen, K. Moth-Poulsen, *Joule* **2021**, *5*, 3116–3136 (DOI: 10.1016/j.joule.2021.11.001).

84 T. P. Mart'yanov, L. S. Klimenko, E. N. Ushakov, Russ. J. Org. Chem. **2016**, *52*, 1126–1136 (DOI: 10.1134/S1070428016080066).

85 (a) J. P. Phillips, A. Mueller, F. Przystal, *J. Am. Chem. Soc.* **1965**, *87*, 4020 (DOI: 10.1021/ja01095a067). (b) J. D. Winkler, C. M. Bowen, V. Michelet, *J. Am. Chem. Soc.* **1998**, *120*, 3237–3242 (DOI: 10.1021/ja974181p). (c) T. J. Feuerstein, R. Müller, C. Barner-Kowollik, P. W. Roesky, *Inorg. Chem.* **2019**, *58*, 15479–15486 (DOI: 10.1021/acs.inorgchem.9b02547).

86 Yu. P. Strokach, V. A. Barachevsky, N. T. Sokolyuk, Yu. E. Gerasimenko, *Khim. Phys.* **1987**, *6*, 320-328 (In Russian).

87 V. I. Binyukov, N. I. Koroteev, S. A. Krikunov, S. A. Magnitskii, D. V. Malakhov, V. V. Shubin, N. T. Sokolyuk, *Jpn. J. Appl. Phys*. **1998**, *37*, 2118-2119 (DOI: 10.1143/JJAP.37.2118).

88 J. Malkin, A. Zelichenok, V. Krongauz, A. S. Dvornikov, P. M. Rentzepis, *J. Am. Chem. Soc.* **1994**, *116*, 1101-1105 (DOI: 10.1021/ja00082a037).

89 Y. Li, B. He, J. Zhang, *Dyes Pigm.* **2007**, *75*, 111-115 (DOI: 10.1016/j.dyepig.2006.05.026).

90 M. Hanazawa, R. Sumiya, Y. Horikawa, M. Irie, *J. Chem. Soc., Chem. Commun.* **1992**, 206-207 (DOI: 10.1039/C39920000206).

91 H. G. Heller, J. R. Langan, *J. Chem. Soc., Perkin Trans. 2* **1981**, 341-343 (DOI: 10.1039/P29810000341).

92 X. Cui, J. Zhao, Y. Zhou, J. Ma, Y. Zhao, *J. Am. Chem. Soc.* **2014**, *136*, 9256−9259 (DOI: 10.1021/ja504211y).

93 T. Sumi, Y. Takagi, A. Yagi, M. Morimoto, M. Irie, *Chem. Commun.* **2014**, *50*, 3928-3930 (DOI: 10.1039/c4cc00396a).

94 E. Uhlmann, G. Gauglitz, *J. Photochem. Photobiolog.* **1996**, *98*, 45-49 (DOI: 10.1016/1010-6030(96)04323-7)

[95] F. Buchholtz, A. Zelichenok, V. Krongauz, *Macromolecules* **1993**, *26*, 906-910 (DOI: 10.1021/ma00057a004).

[96] L. Klimenko, Z. Leonenko, N. Gritsan, *Mol. Cryst. Liq. Cryst.* **1997**, *297*, 181-188 (DOI: 10.1080/10587259708036120).

[97] L. S. Klimenko, N. P. Gritsan, E. P. Fokin, *Bull. Acad. Sci. USSR, Div. Chem. Sci.* **1990**, *39*, 306–310 (DOI: 10.1007/BF00960658).

[98] Z. V. Leonenko, N. P. Gritsan, L. S. Klimenko, *Russ. Chem. Bull.* **1995**, *44*, 247-252 (DOI: 10.1007/BF00702129).

[99] N. P. Gritsan, L. S. Klimenko, Z. V. Leonenko, l. Ya. Mainagashev, V. L Mamatyuk, V. P. Vetchinov, *Tetrahedron* **1995**, *51*, 3061-3076 (DOI: 10.1016/0040-4020(95)00046-B).

[100] S. Park, E. Heo, Y.-S. Nam, C. Woo Lee, J.-M. Kim, *J. Photochem. Photobiol. A* **2012**, *238*, 1-6 (DOI: 10.1016/j.jphotochem.2012.04.003).

[101] N. P. Gritsan, S. A. Russkikh, L. S. Klimenko, V. F. Plyusnin, *Theor. Exp. Chem.* **1984**, *19*, 533–539 (DOI: 10.1007/BF00526026).

[102] S. Y. Ju, K.-D. Ahn, D. K. Han, D. H. Suh, J.-M. Kim, *J. Photosci.* **2000**, *7*, 131-133 (DOI:).

[103] S. Y. Ju, D.-I. Kwon, S.-J. Min, K.-D. Ahn, K. H. Park, J.-M. Kim, *J. Photochem. Photobiolog. A* **2003**, *160*, 151–157 (DOI: 10.1016/S1010-6030(03)00211-9).

[104] K.-D. Ahn, J.-H. Kang, K.-W. Chi, K.-D. Park, C. W. Lee, *Bull. Korean Chem. Soc.* **2009**, *30*, 1243-1244 (DOI: 10.5012/bkcs.2009.30.6.1243).

[105] J.-M. Kim, H.-Y. Shin, K. H. Park, T.-H. Kim, S. Y. Ju, D. K. Han, K.-D. Ahn, *Macromolecules* **2001**, *34*, 4291-4293 (DOI: 10.1021/ma002061n).

[106] A. J. Myles, B. Gorodetsky, N. R. Branda, *Adv. Mat.* **2004**, *16*, 922-925 (DOI: 10.1002/adma.200306227)

[107] For reviews, see: (a) H.-L. Dai, Y.-F. Geng, Q.-D. Zeng, C. Wang, *Chin. Chem. Lett.* **2017**, *28*, 729-737 (DOI: 10.1016/j.cclet.2016.09.018). (b) D. Frath, S. Yokoyama, T. Hirose, K. Matsuda, *J. Photochem. Photobiolog. C* **2018**, *34*, 29-40 (DOI: 10.1016/j.jphotochemrev.2017.12.005).

[108] I. Oreshkin, V.I. Panov, S.I. Vasil'ev, N.I. Koroteev, S.A. Magnitskii, *JETP Lett.* **1998**, *68*, 521–526 (DOI: 10.1134/1.567900).

[109] N.S. Maslova, A.I. Oreshkin, V.I. Panov, S.A. Magnitskii, *Solid State Commun.* **2001**, *117*, 41-46 (DOI: 10.1016/S0038-1098(00)00399-9).

[110] F. Maurela, A. Perriera, D. Jacquemin, *J. Photochem. Photobiol. A* **2011**, *218*, 33–40 (DOI: 10.1016/j.jphotochem.2010.11.021).

[111] A. J. Myles, N. R. Branda, *J. Am. Chem. Soc.* **2001**, *123*, 177-178 (DOI: 10.1021/ja002733p).

[112] L. Jia, G. Zhang, D. Zhang, J. Xiang, W. Xu, D. Zhu, *Chem. Commun.* **2011**, *47*, 322–324 (DOI: 10.1039/C0CC02110E).

[113] Y. Kim, T. J. Hellmuth, D. Sysoiev, F. Pauly, T. Pietsch, J. Wolf, A. Erbe, T. Huhn, U. Groth, U. E. Steiner, E. Scheer, *Nano Lett.* **2012**, *12*, 3736−3742 (DOI: 10.1021/nl3015523).

[114] Jia, C.; Migliore, A.; Xin, N.; Huang, S.; Wang, J.; Yang, Q.; Wang, S.; Chen, H.; Wang, D.; Feng, B.; Liu, Z.; Zhang, G.; Qu, D.-H.; Tian, H.; Ratner, M. A.; Xu, H. Q.; Nitzan, A.; Guo, X., *Science* **2016**, *352*, 1443-1445 (DOI: 10.1126/science.aaf6298).

[115] P. Zhao, D.S. Liu, S.J. Xie, *Phys. Lett. A* **2008**, *372*, 5811–5815 (DOI: 10.1016/j.physleta.2008.07.014).

[116] P. Zhao, C.F. Fang, Y.M. Wang, Y.X. Zhai, D.S. Liu, *Physica E* **2009**, *41*, 474–478 (DOI: 10.1016/j.physe.2008.09.008).

[117] Yu. E. Gerasimenko, N. T. Poteleshchenko, V. V. Romanov, *Zh. Org. Khim.* **1980**, *16*, 2014-2015 (in Russian).

[118] M. B. Nielsen, N. Ree, K. V. Mikkelsen, M. Cacciarini, *Russ. Chem. Rev.* **2020**, *89*, 573-586 (DOI: 10.1070/RCR4944).

[119] D. V. Malakhov, F. E. Gostev, N. I. Koroteev, V. V. Lozovoi, S. A. Magnitskii, O. M. Sarkisov, D. G. Tovbin, A. A. Titov, *Chem. Phys. Rep.* **2000**, *18*, 1217–1232 (D. V. Malakhov, F. E. Gostev, N. I. Koroteev, V. V. Lozovoi, S. A. Magnitskii, O. M. Sarkisov, D. G. Tovbin, A. A. Titov, *Khim. Fiz.* **1999**, *18*, 18–25 (in Russian))

[120] N. P. Gritsan. *Mol. Cryst. Liq. Cryst.* **1997**, *297*, 167-174 (DOI: 10.1080/10587259708036118).

[121] S. Fredrich, A. Bonasera, V. Valderrey, S. Hecht, *J. Am. Chem. Soc.* **2018**, *140*, 6432-6440. (DOI: 10.1021/jacs.8b02982).

[122] I. Sung Park, E.-J. Heo, J.-M. Kim, *Tetrahedron Lett.* **2011**, *52*, 2454–2457 (DOI: 10.1016/j.tetlet.2011.02.105).

[123] L S. Klimenko, S Z. Kusov, V. M. Vlasov, *Mendeleev Commun.* **2002**, *12*, 102–103 (DOI: 10.1070/MC2002v012n03ABEH001592).

[124] T. P. Martyanov, L. S. Klimenko, V. I. Kozlovskiy, E. N. Ushakov, *Tetrahedron* **2017**, *73*, 681-691 (DOI: 10.1016/j.tet.2016.12.048).

[125] T. P. Martyanov, E. N. Ushakov, V. A. Savelyev, L. S. Klimenko, *Russ. Chem. Bull., Int. Ed.* **2012**, *61*, 2282-2294 (DOI: 10.1007/s11172-012-0323-z).

[126] E. J. Son, J. H. Kim, K. Kim, C. B. Park, *J. Mater. Chem. A* **2016**, *4*, 11179–11202 (DOI: 10.1039/C6TA03123D).

[127] J. Bitenc, T. Pavčnik, U. Košir, K. Pirnat, *Materials* **2020**, *13*, 506 (DOI: 10.3390/ma13030506).

[128] A. J. Myles, N. R. Branda, *Tetrahedron Lett.* **2000**, *41*, 3785–3788 (DOI: 10.1016/S0040-4039(00)00503-7).

129 M. V. Peters, R. Goddard, S. Hecht, *J. Org. Chem.* **2006**, *71*, 7846–7849 (DOI: 10.1021/jo0612877).

130 A. Fihey, A. Perrier, W. R. Browned, D. Jacquemin, *Chem. Soc. Rev.* **2015**, *44*, 3719-3759 (DOI: 10.1039/C5CS00137D).

131 A. Perrier, F. Maurel, D. Jacquemin, *Acc. Chem. Res.* **2012**, *45*, 1173–1182 (DOI: 10.1021/ar200214k).

132 G. Zimmerman, L.-Y. Chow, U.-J. Paik, *J. Am. Chem. Soc.* **1958**, *80*, 3528–3531 (DOI: 10.1021/ja01547a010).

133 Z. Fang, H. Zhang, S. Wang, Z. Yang, T. Fang, S. Xu, F. Wang, *Chin. J. Appl. Chem.* **1997**, *14*, 1-5 (in Chinese).

134 A. J. Myles, T. J. Wigglesworth, N. R. Branda, *Adv. Mat.* **2003**, *15*, 745-748 (DOI: 10.1002/adma.200304917).

135 For reviews, see: (a) I. Willner, A. Doron, E. Katz, *J. Phys. Org. Chem.* **1998**, *11*, 546–560 (DOI: 10.1002/(SICI)1099-1395(199808/09)11:8/9<546::AID-POC49>3.0.CO;2-Q). (b) E. Katz, *Electroanalysis* **2018**, *30*, 759-797 (DOI: 10.1002/elan.201800015).

136 A. Doron, M. Portnoy, M. Lion-Dagan, E. Katz, I. Willner, *J. Am. Chem. Soc.* **1996**, *118*, 8937-8944 (DOI: 10.1021/ja961814b).

137 M. Lahav, E. Katz, A. Doron, F. Patolsky, I. Willner, *J. Am. Chem. Soc.* **1999**, *121*, 862-863 (DOI: 10.1021/ja983330g).

138 M. Lahav, E. Katz, I. Willner, *Langmuir* **2001**, *17*, 7387-7395 (DOI: 10.1021/la011172s).

139 C.-Y. Huang, S. Hecht, *Chem. Eur. J.* **2023**, *29*, e202300981 (DOI: 10.1002/chem.202300981).

140 E. Orgiu, P. Samorì, *Adv. Mat.* **2014**, *26*, 1827-1845 (DOI: 10.1002/adma.201304695).

141 (a) Y. Wakayama, R. Hayakawa, K. Higashiguchi, K. Matsuda, *J. Mat. Chem. C* **2020**, *8*, 10956-10974 (DOI: 10.1039/D0TC02683B). (b) C. Xu, J. Zhang, W. Xu, H. Tian, *Mater. Chem. Front.* **2021**, *5*, 1060-1075 (DOI: 10.1039/D0QM00567C).

142 S. Delbaere, G. Vermeersch, *J. Photochem. Photobiol. C* **2008**, *9*, 61-80 (DOI: 10.1016/j.jphotochemrev.2008.04.003).

143 R. Weinstain, T. Slanina, D. Kand, P. Klán, *Chem. Rev.* **2020**, *120*, 13135–13272 (DOI: 10.1021/acs.chemrev.0c00663).

144 (a) N. F. König, D. Mutruc, S. Hecht, *J. Am. Chem. Soc.* **2021**, *143*, 9162–9168 (DOI: 10.1021/jacs.1c03631). (b) D. N. Barsoum, V. C. Kirinda, B. Kang, J. A. Kalow, *J. Am. Chem. Soc.* **2022**, *144*, 10168–10173 (DOI: 10.1021/jacs.2c04658).